2018

Targeting of N-Type Calcium Channels via GABAB-Receptor Activation by α-Conotoxin Vc1.1 Variants Displaying Improved Analgesic Activity

Fengtao Cai
Guangxi Medical University, Beijing Institute of Biotechnology

Ning Xu
Beijing Institute of Biotechnology

Zhuguo Liu
Beijing Institute of Biotechnology

Rong Ding
Beijing Institute of Biotechnology

Shuo Yu
Beijing Institute of Biotechnology

See next page for additional authors

Publication Details

Cai, F., Xu, N., Liu, Z., Ding, R., Yu, S., Dong, M., Wang, S., Shen, J., Tae, H., Adams, D. J.., Zhang, X. & Dai, Q. (2018). Targeting of N-Type Calcium Channels via GABAB-Receptor Activation by α-Conotoxin Vc1.1 Variants Displaying Improved Analgesic Activity. Journal of Medicinal Chemistry, 61 (22), 10198-10205.

Targeting of N-Type Calcium Channels via GABAB-Receptor Activation by α-Conotoxin Vc1.1 Variants Displaying Improved Analgesic Activity

Abstract

α-Conotoxins exhibiting analgesic activity, such as Vc1.1, have been shown to inhibit α9α10 nicotinic acetylcholine receptors (nAChRs) and $GABA_B$-receptor ($GABA_BR$) coupled N-type ($Ca_V2.2$) calcium channels. Here, we report two Vc1.1 variants, Vc1.1[N9R] and benzoyl-Vc1.1[N9R], that selectively inhibit $Ca_V2.2$ channels via $GABA_BR$ activation but exhibit reduced inhibitory activity at α9α10 and other neuronal nAChR subtypes compared with Vc1.1. Surprisingly, the analgesic activity of Vc1.1[N9R] and benzoyl-Vc1.1[N9R] was more potent than that of Vc1.1 when tested in partial sciatic nerve ligation injury and chronic constriction injury models. Vc1.1[N9R] and benzoyl-Vc1.1[N9R] exhibited either similar or tenfold higher activity of $GABA_BR$-mediated $Ca_V2.2$ inhibition but no activity at $Ca_V2.2$ alone; however, the mechanism of increased analgesic activity is unknown. The effects on analgesic activity and α9α10 nAChR of other Vc1.1 variations at position 9 and the N-terminus were also determined. Our findings provide new insights for designing potent inhibitors for $GABA_BR$-coupled N-type ($Ca_V2.2$) calcium channels.

Disciplines

Medicine and Health Sciences

Publication Details

Cai, F., Xu, N., Liu, Z., Ding, R., Yu, S., Dong, M., Wang, S., Shen, J., Tae, H., Adams, D. J.., Zhang, X. & Dai, Q. (2018). Targeting of N-Type Calcium Channels via GABAB-Receptor Activation by α-Conotoxin Vc1.1 Variants Displaying Improved Analgesic Activity. Journal of Medicinal Chemistry, 61 (22), 10198-10205.

Authors

Fengtao Cai, Ning Xu, Zhuguo Liu, Rong Ding, Shuo Yu, Mingxin Dong, Shuo Wang, Jintao Shen, Han Shen Tae, David J. Adams, Xuerong Zhang, and Qiuyun Dai

Targeting of N-type Calcium Channels via $GABA_B$ Receptor activation by α-Conotoxin Vc1.1 Variants Displaying Improved Analgesic Activity

Fengtao Cai,[†,‡] Ning Xu,[†] Zhuguo Liu,[†] Rong Ding,[†] Shuo Yu,[†] Mingxin Dong,[†] Shuo Wang,[†] Jintao Shen,[†] Han-Shen Tae,[§] David J. Adams,[§,*] Xuerong Zhang[‡,*], Qiuyun Dai*,[†]

[†] Beijing Institute of Biotechnology; Beijing 100071, China

[‡] School of Preclinical Medicine, Guangxi Medical University, Nanning 530021, China

[§] Illawarra Health and Medical Research Institute (IHMRI), University of Wollongong, Wollongong, NSW 2522, Australia

Fengtao Cai, Ning Xu, and Zhuguo Liu contributed equally to this work.

ABSTRACT: α-Conotoxins exhibiting analgesic activity have been shown to inhibit α9α10 nicotinic acetylcholine receptors (nAChRs) and $GABA_B$ receptor ($GABA_BR$)-coupled N-type ($Ca_V2.2$) calcium channels. Here, we report two Vc1.1 variants, Vc1.1[N9R] and benzoyl-Vc1.1[N9R], selectively inhibit $Ca_V2.2$ channels via $GABA_BR$ activation but exhibit reduced inhibitory activity at α9α10 and other neuronal nAChR subtypes compared to Vc1.1. Surprisingly, the analgesic activity of Vc1.1[N9R] and benzoyl-Vc1.1[N9R] was more potent than Vc1.1 when tested in the partial sciatic nerve injury and chronic constriction injury models. Vc1.1[N9R] and benzoyl-Vc1.1[N9R] exhibited either similar or ten-fold higher activity of $GABA_BR$-mediated $Ca_V2.2$ inhibition but no activity at $Ca_V2.2$ alone, however, the mechanism of increased analgesic activity is unknown. The effects of other Vc1.1 variants at position 9 and the N-terminus were also determined on analgesic activity and α9α10 nAChR. Our findings provide new insights to design potent inhibitors for $GABA_BR$-coupled N-type ($Ca_V2.2$) calcium channels.

■ INTRODUCTION

Nicotinic acetylcholine receptors (nAChRs) are a diverse family of ligand-gated cation selective channels which are widely distributed in the central and peripheral nervous systems.[1, 2] Some nervous system diseases are involved with nAChR dysfunctions,[3,4] such as neuropathic pain,[5~7] Parkinson's disease,[8, 9] and schizophrenia.[10] Recently, several nAChR subtypes have been identified as potential targets for treatment of neuropathic pain with α-conotoxins.[11-13] A number of α-conotoxins, such as Vc1.1,[14] Rg1A,[15] MII,[16] and AuIB,[17] which are composed of 11-20 amino acids and two disulfide bridges and target α9α10, α3β2

or α3β4 nAChRs, have been shown to possess analgesic activity.

Vc1.1 is the first α-conotoxin to exhibit potent analgesic activity and accelerate the functional recovery of injured neurons,[14] and it entered phase II of clinical studies.[18] Vc1.1 reversibly inhibits α9α10 nAChR and weakly inhibits α3β2 and α3β4 nAChRs.[19, 20] Vc1.1 also potently inhibits N-type ($Ca_V2.2$) Ca^{2+} channels via $GABA_BR$ activation.[21] The co-administration of a selective $GABA_BR$ antagonist with Vc1.1 in rats completely abolishes its analgesic action, suggesting that the analgesic activity of Vc1.1 is mediated by $GABA_BR$ activation. However, to date, α-conotoxins which exhibit potent analgesic activity are largely inhibitors of α9α10 nAChR and $GABA_BR$-coupled $Ca_V2.2$ channels.[22, 23]

In the primary screening of analgesic activity of Vc1.1 variants, the modifications at position 9 affected Vc1.1's analgesic activity, and the substitution of Asn9 with Arg improved the analgesic activity of Vc1.1 in rat partial sciatic nerve injury (PNL). Therefore, in the present study, we investigated the effects of charge and hydrophobic features at N-terminal and position 11 on the analgesic activity of Vc1.1[N9R]. The structure-activity relationship of these variants on α9α10 nAChR and $GABA_BR$-coupled $Ca_V2.2$ channels were determined. The results showed that benzoyl-Vc1.1[N9R] apparently improved analgesic activities as Vc1.1[N9R] in rat PNL and chronic constriction injury model (CCI) compared to Vc1.1, whereas their inhibitory activity at α9α10 nAChR were 29- and 172-fold lower than that of Vc.1. In contrast, the two Vc1.1 variants displayed similar or ten-fold higher inhibitory activity at $Ca_V2.2$ channels in HEK293T cells co-expressed with $GABA_BR$ but not $Ca_V2.2$ alone. The results demonstrate that the target specificity of two Vc1.1 variants is significantly different from that of Vc1.1. However, the further replacement of Asp11 by Asn

or acetylation at the N-terminus of Vc1.1[N9R] significantly reduced the inhibitory activity at the rat α9α10 nAChR and $GABA_BR$-coupled $Ca_V2.2$. These findings provide new insights into designing potent inhibitors for $GABA_BR$-coupled $Ca_V2.2$ channels.

■ RESULTS

Chemical Synthesis and Characterization of Vc1.1 Variants. Linear Vc1.1 and its variants (Table 1) were folded individually in NH_4HCO_3 buffer and analyzed by HPLC. The typical folding results of Vc1.1[N9R] and benzoyl-Vc1.1[N9R] are shown in Figure 1, other Vc1.1 variants are shown in Figures S8-S16; all linear Vc1.1 and its variants folded to form a major product. The resulting peptides were further purified and assessed with analytical reversed-phase HPLC, and the purity of the peptides was determined as ≥ 95% (Figure S8-S16). The mass spectral analysis showed that Vc1.1 and variants were the correct folded products (Figure S17-S25). The circular dichroism (CD) spectra of Vc1.1 and its variants in 0.01 M phosphate buffer showed some ellipticities around 208 nm and 220 nm (Figure S26-S34). These results are consistent with previous reports that α4/7-conotoxins have a short helical structure if they have the disulfide bridges C^1-C^3, C^2-C^4 and a conserved proline residue exists in loop 2.[12,19] Thus, this structural feature was used to confirm the disulfide bridges of Vc1.1 variants.

Effect of Residues at Position 9 and 11 on the Analgesic Activity of Vc1.1. The analgesic activity of Vc1.1 and its variants at position 9 and 11 was assessed using rat PNL and CCI models. In the PNL model, ipsilateral Vc1.1[N9R] injection (0.3, 1.5 and 15 nmol/kg) increased the pain threshold elevation percentages by 16.7 ± 10.0% , 47.2 ± 17.8% and 85.0 ± 30.0% (n = 8), respectively, in a dose-dependent manner (Figure 2A), and was

higher than Vc1.1 at the same dose, which increased the pain threshold elevation percentages by 12.2 ± 14.4%, 25.6 ± 19.4% and 51.1 ± 21.1% (n = 8), respectively. The same tendency was observed in rat CCI model (Figure 2B). Next, the analgesic effect of residues at position 11 on Vc1.1[N9R] was assessed. The replacement of Asp at position 11 with Arg, Ser or Asn led to decreased analgesic activity in Vc1.1[N9R, D11R], Vc1.1[N9R, D11S] and Vc1.1[N9R, D11N], in which the pain threshold elevation percentages were 35.3 ± 20.0%, 9.0 ± 22.5% and 40.8 ± 21.5% (n = 8), respectively (Figure S1), whereas the value for Vc1.1 and Vc1.1[N9R] was 58.8 ± 17.5% and 83.8 ± 29.5% (n = 8), respectively, in the same experiment. These results demonstrate that the residue at position 11 is also important for the analgesic properties of Vc1.1[N9R].

Effect of N-terminal Modification on Vc1.1[N9R] Analgesic Activity. The N-terminus of Vc1.1[N9R] was further modified with benzoyl, acetyl or other amino acids, and the analgesic activity was determined in PNL and CCI rats. When benzoyl was introduced to the N-terminal of Vc1.1[N9R], the analgesic activity remained higher than that of unmodified Vc1.1 (Figure 3). At a dose of 15 nmol/kg, benzoyl-Vc1.1[N9R] increased the pain threshold to 80.0 ± 17.3%, approximately 72% higher than Vc1.1 (46.4 ± 10.0%) (Figure 3A). A similar effect was observed in CCI model rats (Figure 3B). N-terminal acetyl (Ac) modification or Gly deletion (Des-Gly) from the N-terminus of Vc1.1[N9R] both negatively affected analgesic activity, although the activities of these modified peptides were comparable with Vc1.1 in PNL rats (Figure S2).

Potency of Vc1.1 Variants at nAChR Subtypes. Two-electrode voltage clamp was used to assess the effects of Vc1.1 variants on ACh-evoked currents of nAChR subunits

expressed in *Xenopus laevis* oocytes. The inhibitory activity of Vc1.1 and several variants at rat and human α9α10 nAChRs is shown in Figure 4 and Figure S3, respectively. The IC_{50} obtained for inhibition of rat α9α10 nAChR by Vc1.1, Vc1.1[N9R] and benzoyl-Vc1.1[N9R] was 28.3 nM, 4901 nM, and 875 nM, respectively (Table 1). The replacement of Asn9 by Arg and its further benzoylation at N-terminus resulted in a 29- and 172-fold reduction, respectively, in the inhibitory activity of the peptide at rat α9α10 nAChRs. The IC_{50}'s obtained for inhibition of human α9α10 nAChR by Vc1.1[N9R], benzoyl-Vc1.1[N9R] and benzoyl-Vc1.1 were 363 nM, 5.93 μM, and 12.50 μM, respectively (Table 1).

Furthermore, the inhibition of rat α3β2, α3β4, α2β4, α2β2, α4β2 and α7 by 10 μM Vc1.1[N9R] and benzoyl-Vc1.1[N9R] was reduced by ≥ 50% (Figure S4-S5). These results indicate that the analgesic activity of Vc1.1[N9R] and benzoyl-Vc1.1[N9R] is unlikely to be due its inhibitory activity at α9α10 or other neuronal nAChR subtypes. Similarly, the replacement of Asn9 with Asp, the acetylation of [N9R]Vc.1 at N-terminus and the substitution of Asn9 and Asp11 with Arg and Asn, respectively, led to significant decrease in the potency of Vc1.1 at rat α9α10 nAChR (Figure 4B). At human α9α10, Vc1.1[N9R] was ~3 times more potent than Vc1.1 (IC_{50} = 1 μM)[24] (Table 1) .

Potency of Vc1.1 Variants at $GABA_BR$-coupled $Ca_V2.2$ Channels. The inhibitory activity of Vc1.1 variants on $Ca_V2.2$ channels in HEK293T cells co-expressed with $GABA_BR$ was also investigated. Vc1.1[N9R] and benzoyl-Vc1.1[N9R] inhibited $Ca_V2.2$ channels via $GABA_BR$ activation to similar degree or greater with an IC_{50}s of 4.9 nM and 0.2 nM, respectively, compared to 2.4 nM for Vc1.1 (Figure 5F). The effects of the three peptides were antagonized in the presence of 1 μM CGP55845 (n = 4), a selective $GABA_BR$

antagonist, and a representative effect of benzoyl-Vc1.1[N9R] on HEK293T cells coexpressing $GABA_BR$ and $Ca_V2.2$ is shown in Figure 5E. In addition, benzoyl-Vc1.1[N9R] was inactive in HEK293T cells expressing $Ca_V2.2$ alone (Figure 5E). However, further substitutions of Asp with Asn, Ser and Arg or acetylation or deletion of first amino acid at N-terminal resulted in a decrease in inhibitory activity (Figure 5H-5G). Similar to benzoyl-Vc1.1[N9R], single modifications of benzoylation at the N-terminal led to an increase in potency (Figure 5H). Furthermore, the three peptides, Vc1.1, Vc1.1[N9R] and benzoyl-Vc1.1[N9R], tested at a concentration of 10 μM had no significant effect on either TTX-resistant (TTX-R; Figure S6) or TTX-sensitive sodium channels (TTX-S; Figure S7) in rat DRG neurons. These results suggest that Vc1.1[N9R] and benzoyl-Vc1.1[N9R] specifically inhibit $GABA_BR$-coupled $Ca_V2.2$ channels.

■ DISCUSSION

According to the residue numbers of the inter cysteine loops (-CC-(loop1)-C-(loop2)-C-), α-conotoxins are divided into several subfamilies (α3/5, α4/3, α4/4, α4/6, α4/7 and α5/5).[12] ImI and Rg1A belong to the α4/3 subfamily, whereas PnIA, PnIB and Vc1.1 belong to the α4/7 subfamily. Mutagenesis studies of α-conotoxins ImI, Rg1A, PnIA, PnIB and Vc1.1 have shown that loop 1 of α-conotoxin plays a key role in recognizing nAChR subtypes and that loop 2 is important to both activity and selectivity.[25-32] Mutations of Asp5-Arg7 and Asp11-Ile15 in Vc1.1 resulted in loss of activity at rat α9α10 nAChR.[33] However, replacing the polar residue Asn9 with a hydrophobic residue such as Leu, Ile, Phe or Trp significantly increased the potency of Vc1.1 at both the rat α9α10 and the human/rat α9α10 hybrid nAChRs.[32-35] In the present study, substitution of Asn9 with Arg in Vc1.1, the further

replacement of Asp11 by Asn or acetylation at the N-terminus of Vc1.1[N9R] significantly reduced the inhibitory activity at the rat α9α10 nAChR, which is consistent with a previous report that substitution of Asn9 with Lys reduced Vc1.1 activity.[34]

Surprisingly, the substitution of Asn9 with Arg in Vc1.1 and further benzoylation at the N-terminus apparently increased analgesic activity (Figure 2-3). These results suggest that the analgesic activity of Vc1.1[N9R], benzoyl-Vc1.1[N9R] is not due to their reduced inhibitory activity at α9α10 nAChR. Similar examples are found in Vc1.1 post-translationally modified analogues, such as Vc1a, Vc1.1[P6O] and Vc1.1[E14γ],[32] which are equipotent at inhibiting α9α10 nAChR but lack analgesic activity *in vivo*.

It has been reported that α-contoxins Vc1.1,[21] Rg1A,[15, 36] PeIA,[37] AuIB[17] and Vc1.2[38] also inhibit $GABA_B$R-coupled N-type ($Ca_V2.2$) calcium channels. The discrepancy between the inhibitory activity of Vc1.1[N9R] and benzoyl-Vc1.1[N9R] at α9α10 nAChR and analgesic activity led to the demonstration of their potent inhibition of $GABA_B$R-coupled $Ca_V2.2$ channels in HEK293T cells. Our results showed that Vc1.1[N9R] exhibited similar inhibitory activity at $GABA_B$R-coupled Cav2.2 channels as Vc1.1 whereas benzoyl-Vc1.1 and benzoyl-Vc1.1[N9R] are 1- and 10-fold more potent than Vc1.1 (Figure 5). To our knowledge, benzoyl-Vc1.1[N9R] is the most potent inhibitor of $GABA_B$R-coupled $Ca_V2.2$ channels. In addition, Vc1.1 and the two variants (10 μM) exhibited no significant effect on $Ca_V2.2$ expressed alone in HEK293T cells, nor TTX-R (Figure S6) and TTX-S Na^+ channels (Figure S7) in rat DRG neurons. The effect of benzoyl-Vc1.1[N9R] was antagonized in the presence of the selective $GABA_B$ receptor antagonist, CGP55845. However, the analgesic activity of Vc1.1 and Vc1.1[N9R] is not strictly coupled to its potency at $GABA_B$R/$Ca_V2.2$

channels. The *in vitro* degradation of two peptides (data not shown) appears to exclude the possible effects of pharmacokinetics *in vivo*, but the mechanism of increased analgesic activity is unknown.

In conclusion, the substitution of Asn9 with Arg, or the further modification of the N-terminus with a benzoyl group improves Vc1.1 analgesic activity. Our findings will be valuable for designing new potent inhibitors for $GABA_BR$-coupled $Ca_V2.2$ channels.

■ EXPERIMENTAL SECTION

Animals. Adult male Sprague-Dawley rats (SD, 200-220 g, 6-7 week old) (Beijing Animal Center, China) were housed in groups of eight on a 12 h light-dark cycle (light cycle from 8 AM – 8 PM) at a temperature of 23 ± 2 °C and a relative humidity of 50%. Food pellets and water were available *ad libitum*. All experiments were conducted in accordance with the guidelines of the Beijing Institutes for Biological Sciences Animal Research Advisory Committee and conformed to the European Community directives for the care and use of laboratory animals.

Reagents. N-Fmoc-amino acids, HOBt, HBTU, DIEA and TFA were purchased from GL Biochem Ltd. (Shanghai, China). Wang resin and Rink resin were obtained from Tianjin Nankai Hecheng S&T Co. (China). DTT was obtained from Promega. Baclofen and GABA were purchased from Aladdin Reagent (Shanghai, China). All other reagents were of analytical grade. Human $GABA_{B1}R$ and $GABA_{B2}R$ subunit cDNA clones were obtained from OriGene Technologies, Inc. (Rockville, MD, USA). The rat $Ca_V2.2$ channel α_{1B} splice variant e37a, and auxiliary subunits β3 and $\alpha_2\delta1$ were obtained from Addgene (Cambridge, MA,

USA).

Peptide Synthesis and Folding. Vc1.1 and its variants (Table 1) were synthesized using the solid-phase method on an ABI 433A peptide synthesizer (Thermo Fisher Scientific) using standard Fmoc chemistry and side-chain protection as described previously.[39,40] The lyophilized crude linear peptide was folded in 0.1M NH_4HCO_3 buffer (pH 8.2~8.4) at concentration of 0.3 mg/mL in an open flask for 38 h.

Following oxidation of the peptide, the reaction mixture was acidified (pH < 4.5) with acetic acid and loaded on a Nucleosil 25×250 mm preparative C18 column using a preparative HPLC pump (Waters Delta Prep 4000). The column was washed with 95% acetonitrile containing 0.1% TFA at a flow rate of 5.0 mL/min. The resulting peptide was further purified by semi-preparative reversed-phase HPLC using a 10×250 mm Kromasil C18 column. The purity of the peptide was assessed by analytical reversed-phase HPLC using a Calesil C_{18} column (5 μm, 100 Å, 4.6×250 mm) with a 25 min linear gradient of 8-40% buffer B (0.1% TFA in acetonitrile) at a flow rate of 1 mL/min. The purity of all final products was of ≥ 95% . Confirmation that the product was of the correct molecular mass was obtained by mass spectrometry on a ProFLEXTM-III MALDI-TOF spectrometer.

Circular Dichroism (CD) Spectra. CD spectra of Vc1.1 and its variants were measured between 190 and 340 nm on Chirascan-plus CD (Applied Photophysics ltd., Leatherhead, UK). The peptide was dissolved in 0.01 M phosphate buffer (pH 7.2) to a final concentration of 35 μM. A 1-mm path length quartz cell was employed. Each spectrum represented the accumulation of three individual scans collected at 1.0 nm intervals at a bandwidth of 1.0 nm.

Analgesic Activity Test. Under pentobarbital (48 mg/kg) anesthesia, partial sciatic

nerve injury (PNL) was established according to the method of Seltzer[41,42] and chronic constriction injury model (CCI) was achieved using the CCI model of Bennett and Xie.[43,44] All behavioral testing was performed seven days after surgery. A successful PNL model was defined by a 30-50% decrease in mechanical paw withdrawal thresholds (PWT) for the ipsilateral hind paw. Mechanical paw withdrawal thresholds were assessed using an Ugo Basile Analgesy-Meter (Ugo Basile, Italy).

For pharmacological testing, all drugs were dissolved in sterile 0.9% saline. The qualified PNL rats and CCI rats (a 30-50% decrease in PWT) were randomly divided into peptide groups and a saline group with 8 animals in each group. Saline or Vc1.1 (0.3, 1.5 and 15 nmol/kg or single dose) or Vc1.1 variants (0.3, 1.5 and 15 nmol/kg or single dose) was administered ipsilaterally close to the injury site at a mid-thigh region of mice in a volume of 200 μL. The number of groups including a saline and Vc1.1 control group in each experiment was no more than 7. Paw withdrawal thresholds were measured at 2-2.5 h following intramuscular administration. Data are expressed as mean pain threshold elevation percentages (PTEPs) ± SD (%PTEP = (Post-drug PWT-Pre-drug PWT)/ Pre-drug PWT×100). The unpaired t test was performed, and a p value of < 0.05 was considered statistically significant.

Two-electrode Voltage Clamp. cRNA preparation, oocyte harvesting and expression of nAChR subunits and oocyte electrophysiology were performed as described previously.[38,39] Briefly, the *Xenopus laevis* oocytes were incubated in ND96 solution (96.0 mM NaCl, 2.0 mM KCl, 1.8 mM $CaCl_2$, 1.0 mM $MgCl_2$ and 5 mM HEPES, pH ~ 7.3) containing 2.5 mM pyruvic acid sodium (Sigma, St. Louis, MO, USA) and antibiotics (100 U/mL penicillin,

100 mg/mL streptomycin, Sigma) at 18°C. Oocyte recordings were performed 2-4 days post-injection at room temperature (~ 22°C). The oocyte was perfused with peptide solution until equilibrated (5-10 min). At high concentrations (1 μM or greater), 5.5 μL of a 10-fold concentrated peptide solution was directly pipetted into static bath 5 min prior to the exposure of ACh pulses. The concentration-response relationships were fit to the equation: % response = 100/[1 + ([toxin]/IC_{50})n], where n is the Hill coefficient and IC_{50} is the antagonist concentration giving half-maximal response, by non-linear regression analysis using GraphPad Prism (GraphPad Software, San Diego, CA, USA).

HEK293T Cell Electrophysiology. HEK293T cells were seeded into 12 well plates and transiently cotransfected with human $GABA_{B1}$ and $GABA_{B2}$ subunits (2 μg each) and 0.2 μg mCherry fluorescent protein using Lipofectamine 2000 (Invitrogen) according to the manufacturer's protocol. After 24 hours, the cells were then transiently cotransfected with rat $Ca_V2.2$ channels (α_{1B}, β3, and α2δ1 subunits with 1 μg each) and 0.2 μg of the enhanced green fluorescent protein using Lipofectamine 2000 as well.

Two to three days after transfection, cells were seeded on glass coverslips pretreated with poly-L-lysine and incubated at 37°C in 5% CO_2 for at least 6 hours before recording. Whole-cell patch clamp recording from transfected HEK293T cells was performed as described previously.[23, 37] Briefly, HEK293T cells were superfused with a solution containing (in mM): 90 NaCl, 10 $BaCl_2$, 5 CsCl, 30 TEA-Cl, 1 $MgCl_2$, 10 D-glucose, and 10 HEPES, pH 7.4 with TEA-OH. Fire-polished borosilicate patch pipettes (2–3 MΩ tip resistance) were filled with a solution containing (in mM): 120 K-gluconate, 5 NaCl, 2 $MgCl_2$, 5 EGTA, 2 MgATP, 0.6 Na_2GTP, and 10 HEPES, pH 7.2 with CsOH. Whole-cell patch clamp recordings

were performed at room temperature (23–25°C) using a MultiClamp 700B amplifier (Molecular Devices) controlled by Clampex 10.3/DigiData 1440A acquisition systems. Membrane currents were filtered at 2 kHz and sampled at 10 kHz. Leak and capacitive currents were subtracted using a –P/4 pulse protocol. Peak current amplitude in response to the depolarizing pulse was measured once a steady state was achieved (3–5 minutes). All drugs were diluted to the appropriate final concentration and applied via perfusion. Baclofen was used as a positive control for functional expression of $GABA_BR$ with $Ca_V2.2$ channels and cells responding to baclofen with ≥ 50% peak current inhibition were included in our analysis. The concentration-response data were fit to the equation: $Y=Y_{min} + (Y_{min} - Y_{max})/(1+10^{(Log\ IC_{50}-X)}\times h))$, where Y is I/I_0, h is the Hill coefficient (slope), IC_{50} is the half-maximal inhibitory concentration. The non-linear regression analysis was performed using GraphPad Prism (GraphPad Software, San Diego, CA, USA).

■ ASSOCIATED CONTENT

Ⓢ Supporting Information

The Supporting Information is available free of charge on the ACS Publications website at DOI: 10.1021/acs.jmedchem.

Additional information about the analgesic and electrophysiological activities of Vc1.1 variants as well as HPLC analyses and mass spectroscopy of peptides (PDF)

■ AUTHOR INFORMATION

Corresponding Author

*Phone: 86-10-66948897. Fax: 86-10-63833521. E-mail: qy_dai@yahoo.com; Xuerong Zhang, E-mail: zxrsv@126.com; David J. Adams, Email: djadams@uow.edu.au

ORCID

Qiuyun Dai: 0000-0003-2062-8332

David J. Adams: 0000-0002-7030-2288

Author Contributions

F.C., Z.L, R.D., X.Z., J.S., S.W. and H-S.T. synthesized peptides and performed electrophysiological experiments. N.X., M.D. and S.Y. ran analgesic tests. D.J.A. guided electrophysiological experiments and edited the manuscript. Q.D. designed the project and wrote the manuscript.

Notes

The authors declare no conflicts of interests.

■ ACKNOWLEDGMENTS

We are grateful to Prof. Zhonghua Liu (Hunan Normal University) and Dr. Yunxiao Zhang who tested the activities of the peptides on voltage-gated sodium channels in rat DRG neurons**.** This work was supported by the China Natural Science foundation (No. 90713028) and Grant 2010CB529802 from the Basic Research program of China and a National Health & Medical Research Council of Australia Program Grant to D.J.A. (APP1072113)

■ ABBREVIATIONS USED

nAChR, nicotinic acetylcholine receptor; $GABA_BR$, G protein-coupled $GABA_B$ receptor; IC_{50}, half-maximal inhibitory concentration; TFA, trifluoroacetic acid; RP-HPLC, reversed-phase high-performance liquid chromatography; ESI-MS, electrospray-mass spectroscopy; HOBt, 1-hydroxybenzotriazole; DIEA, diisopropylethylamine; HBTU, 2-(1H-benzotriazol-1-yl)-1,1,3,3-tetramethyluronium hexafluorophosphate; Fmoc, N-(9-fluorenyl)methyloxy-carbonyl

■ REFERENCES

(1) Zoli, M.; Pistillo, F.; Gotti, C. Diversity of native nicotinic receptor subtypes in mammalian brain. *Neuropharmacology*. **2015**, *96*, 302-311.

(2) Kutlu, M. G.; Gould, T. J. Nicotinic receptors, memory, and hippocampus. *Curr. Top. Behav. Neurosci.* **2015**, *23*, 137-163.

(3) Dineley, K. T.; Pandya, A. A.; Yakel, J. L. Nicotinic ACh receptors as therapeutic targets in CNS disorders. *Trends. Pharmacol. Sci*. **2015,** *36*, 96-108.

(4) Fuenzalida, M.; Pérez, M. Á.; Arias, H. R. Role of nicotinic and muscarinic receptors on synaptic plasticity and neurological diseases. *Curr. Pharm. Des*. **2016,** *22*, 2004-2014.

(5) Umana, I. C.; Daniele, C. A.; McGehee, D. S. Neuronal nicotinic receptors as analgesic targets: it's a winding road. *Biochem. Pharmacol.* **2013,** *86*,1208-1214.

(6) Hone, A. J.; Servent, D.; McIntosh, J. M. α9-Containing nicotinic acetylcholine receptors and the modulation of pain. *Br. J. Pharmacol*. **2018,** *175*, 1915-1927.

(7) Hone, A. J.; McIntosh, J. M. Nicotinic acetylcholine receptors in neuropathic and inflammatory pain. *FEBS. Lett*. **2018**, *592*, 1045-1062.

(8) Quik, M.; Zhang, D.; McGregor, M.; Bordia, T. Alpha7 nicotinic receptors as therapeutic

targets for Parkinson's disease. *Biochem. Pharmacol.* **2015,** *97*, 399-407.

(9) Jurado-Coronel, J. C.; Avila-Rodriguez, M.; Capani, F.; Gonzalez, J.; Moran, V. E.; Barreto, G. E. Targeting the nicotinic acetylcholine receptors (nAChRs) in astrocytes as a potential therapeutic target in Parkinson's disease. *Curr. Pharm. Des.* **2016,** *22*, 1305-1311.

(10) Parikh, V.; Kutlu, M.G.; Gould ,T.J. nAChR dysfunction as a common substrate for schizophrenia and comorbid nicotine addiction: Current trends and perspectives. *Schizophr. Res.* **2016**, *171*, 1-15.

(11) Dutertre, S.; Nicke, A.; Tsetlin, V. I. Nicotinic acetylcholine receptor inhibitors derived from snake and snail venoms. *Neuropharmacology.* **2017,** *127*, 196-223.

(12) Lebbe, E. K.; Peigneur. S.; Wijesekara, I.; Tytgat, J. Conotoxins targeting nicotinic acetylcholine receptors: an overview. *Mar. Drugs.* **2014,** *12*, 2970-3004.

(13) Chhabra, S.; Belgi, A.; Bartels, P.; van Lierop, B. J.; Robinson, S. D.; Kompella, S. N.; Hung, A.; Callaghan, B. P.; Adams, D. J.; Robinson, A. J.; Norton, R. S. Dicarba analogues of α-conotoxin RgIA. Structure, stability, and activity at potential pain targets. *J. Med. Chem.* **2014,** 57, 9933-9944.

(14) Satkunanathan, N.; Livett, B.; Gayler, K.; Sandall, D.; Down, J.; Khalil, Z. α-Conotoxin Vc1.1 alleviates neuropathic pain and accelerates functional recovery of injured neurons. *Brain. Res.* **2005,** *1059*, 149-158.

(15) Callaghan, B.; Haythornthwaite, A.; Berecki, G.; Clark, R. J.; Craik, D. J.; Adams, D. J. Analgesic α-conotoxins Vc1.1 and Rg1A inhibit N-type calcium channels in rat sensory neurons via $GABA_B$ receptor activation. *J. Neurosci.* **2008,** *28*, 10943–10951.

(16) Young, T.; Wittenauer, S.; McIntosh, J. M.; Vincler, M. Spinal α3β2 nicotinic acetylcholine receptors tonically inhibit the transmission of nociceptive mechanical stimuli. *Brain. Res.* **2008,** *1229*, 118-124.

(17) Napier, I. A.; Klimis, H.; Rycroft, B. K.; Jin, A. H.; Alewood, P. F.; Motin, L.; Adams, D.

J.; Christie, M. J. Intrathecal α-conotoxins Vc1.1, AuIB and MII acting on distinct nicotinic receptor subtypes reverse signs of neuropathic pain. *Neuropharmacology.* **2012,** *62*, 2202-2207.

(18) Gayler, K.; Sandall, D.; Greening, D.; Keays, D.; Polidano, M.; Livett, B.; Down, J.; Satkunanathan, N.; Khalil, Z. Molecular prospecting for drugs from the sea. Isolating therapeutic peptides and proteins from cone snail venom. *IEEE. Eng. Med. Biol Mag.* **2005,** *24*, 79–84.

(19) Clark, R. J.; Fischer, H.; Nevin, S. T.; Adams, D. J.; Craik, D. J. The synthesis, structural characterization and receptor specificity of the α-conotoxin Vc1.1. *J. Biol. Chem.* **2006,** *281*, 23254-23263.

(20) Vincler, M.; Wittenauer, S.; Parker, R.; Ellison, M.; Olivera, B. M., McIntosh, J. M. Molecular mechanism for analgesia involving specific antagonism of α9α10 nicotinic acetylcholine receptors. *Proc. Natl. Acad. Sci. U S A.* **2006,** *103*, 17880–17884.

(21) Klimis, H.; Adams, D. J.; Callaghan, B.; Nevin, S.; Alewood, P. F.; Vaughan, C. W.; Mozar, C. A.; Christie, M. J. A novel mechanism of inhibition of high-voltage activated calcium channels by α-conotoxins contributes to relief of nerve injury-induced neuropathic pain. *Pain.* **2011,** *152*, 259-266.

(22) Adams, D. J.; Callaghan, B.; Berecki, G. Analgesic conotoxins: block and G protein-coupled receptor modulation of N-type ($Ca_V2.2$) calcium channels. *Br. J. Pharmacol.* **2012,** *166*, 486-500.

(23) Huynh, T. G.; Cuny, H.; Slesinger, P. A.; Adams, D. J. Novel mechanism of voltage-gated N-type ($Ca_V2.2$) calcium channel inhibition revealed through α-conotoxin Vc1.1 activation of the $GABA_B$ receptor. *Mol. Pharmacol.* **2015,** *87*, 240-250.

(24) Yu, R., Tae, H-S., Tabassum, N., Shi, J., Jiang. T., Adams. D. J. Molecular determinants conferring the stoichiometric-dependent activity of α-conotoxins at the human α9α10

nicotinic acetylcholine receptor subtype. *J Med Chem.* **2018**, 61(10), 4628-4634.

(25) Quiram, P. A.; Sine, S. M.; Structural elements in α-conotoxin ImI essential for binding to neuronal α7 receptors. *J. Biol. Chem.* **1998,** *273,* 11007-11011.

(26) Ellison, M.; Feng, Z. P.; Park, A. J.; Zhang, X.; Olivera, B. M. McIntosh, JM. Alpha-Rg1A, a novel conotoxin that blocks the α9α10 nAChR: structure and identification of key receptor-binding residues. *J. Mol. Biol.* **2008,** *377,* 1216–1227.

(27) Akondi, K. B.; Muttenthaler, M.; Dutertre, S.; Kaas, Q.; Craik, D. J.; Lewis, R. J.; Alewood, P. F. Discovery, synthesis, and structure-activity relationships of conotoxins. *Chem. Rev.* **2014,** 114, 5815-5847.

(28) Millard, E. L., Daly, N. L.; Craik, D. J. Structure-activity relationships of α-conotoxins targeting neuronal nicotinic acetylcholine receptors. *Eur. J. Biochem.* **2004,** *271,* 2320-2326.

(29) Halai, R.; Callaghan, B.; Daly, N. L.; Clark, R. J.; Adams, D. J.; Craik, D. J. Effects of cyclization on stability, structure, and activity of α-conotoxin RgIA at the α9α10 nicotinic acetylcholine receptor and $GABA_B$ receptor. *J. Med. Chem.* **2011,** *54,* 6984-6992.

(30) Chang, Y. P.; Banerjee, J.; Dowell, C.; Wu, J.; Gyanda, R.; Houghten, R. A.; Toll, L.; McIntosh, J. M.; Armishaw, C. J. Discovery of a potent and selective α3β4 nicotinic acetylcholine receptor antagonist from an α-conotoxin synthetic combinatorial library. *J. Med. Chem.* **2014,** *57,* 3511-3521.

(31) Nevin, S. T.; Clark, R. J.; Klimis, H.; Christie, M. J.; Craik, D. J.; Adams, D. J. Are α9α10 nicotinic acetylcholine receptors a pain target for α-conotoxins? *Mol. Pharmacol.* **2007,** *72,* 1406-1410.

(32) Halai, R.; Clark, R. J.; Nevin, S. T.; Jensen, J. E.; Adams, D. J.; Craik, D. J. Scanning mutagenesis of α-conotoxin Vc1.1 reveals residues crucial for activity at the α9α10 nicotinic acetylcholine receptor. *J. Biol. Chem.* **2009,** *284,* 20275-20284.

(33) Yu, R.; Kompella, S. N.; Adams, D. J.; Craik, D. J.; Kaas, Q. Determination of the

α-conotoxin Vc1.1 binding site on the α9α10 nicotinic acetylcholine receptor. *J. Med. Chem.* **2013,** *56,* 3557-3567.

(34) Indurthi, D. C.; Pera, E.; Kim, H. L.; Chu, C.; McLeod, M. D.; McIntosh, J. M.; Absalom, N. L.; Chebib, M. Presence of multiple binding sites on α9α10 nAChR receptors alludes to stoichiometric-dependent action of the α-conotoxin, Vc1.1. *Biochem. Pharmacol.* **2014,** *89,* 131-140.

(35) Chhabra, S.; Belgi, A.; Bartels, P.; van Lierop, B. J.; Robinson, S. D.; Kompella, S. N.; Hung, A.; Callaghan, B. P.; Adams, D. J.; Robinson, A. J.; Norton, R. S. Dicarba analogues of α-conotoxin RgIA. Structure, stability, and activity at potential pain targets. *J. Med. Chem.* **2014,** *57,* 9933-9944.

(36) Daly, N. L.; Callaghan, B.; Clark, R. J.; Nevin, S. T.; Adams, D. J.; Craik, D. J. Structure and activity of α-conotoxin PeIA at nicotinic acetylcholine receptor subtypes and $GABA_B$ receptor-coupled N-type calcium channels. *J. Biol Chem.* **2011,** *286,* 10233-10237.

(37) Carstens, B. B.; Berecki, G.; Daniel, J. T.; Lee, H. S.; Jackson, K. A., Tae, H. S.; Sadeghi, M.; Castro, J.; O'Donnell, T.; Deiteren, A.; Brierley, S. M.; Craik, D. J.; Adams, D. J.; Clark, R. J. Structure-activity studies of cysteine-rich α-conotoxins that inhibit high voltage-activated calcium channels via $GABA_B$ receptor activation reveal a minimal functional motif. *Angew. Chem. Int. Ed. Engl.* **2016,** *55,* 4692-4696.

(38) Wang, S.; Zhao, C.; Liu, Z.; Wang, X.; Liu, N.; Du, W.; Dai, Q. Structural and functional characterization of a novel α-conotoxin Mr1.7 from *Conus marmoreus* targeting neuronal nAChR α3β2, α9α10 and α6/α3β2β3 subtypes. *Mar. Drugs.* **2015,** *13,* 3259-3275.

(39) Wang, S.; Du, T.; Liu, Z.; Wang, S.; Wu, Y.; Ding, J.; Jiang, L.; Dai, Q. Characterization of a T-superfamily conotoxin TxVC from *Conus textile* that selectively targets neuronal nAChR subtypes. *Biochem. Biophys. Res. Commun.* **2014,** *454,* 151-156.

(40) Seltzer, Z.; Dubner, R.; Shir, Y. A novel behavioral model of neuropathic pain disorders

produced in rats by partial sciatic nerve injury. *Pain.* **1990,** *43,* 205-218.

(41) Wang, F.; Yan, Z.; Liu, Z.; Wang, S.; Wu, Q.; Yu, S.; Ding, J.; Dai, Q.Y. Molecular basis of toxicity of N-type calcium channel inhibitor MVIIA. *Neuropharmacology.* **2016,** *101,* 137-145.

(42) Bennett, G. J.; Xie, Y. K. A peripheral mononeuropathy in rats that produce disorders of pain sensation like those seen in men. *Pain.* **1988,** *33,* 87-107.

(43) Liu, Z.; Bartels, P.; Sadeghi, M.; Du, T.; Dai, Q.; Zhu, C.; Yu, S.; Wang, S.; Dong, M.; Sun, T.; Guo, J.; Peng, S.; Jiang, L.; Adams, D. J.; Dai, Q. Y. A novel α-conopeptide Eu1.6 inhibits N-type ($Ca_V2.2$) calcium channels and exhibits potent analgesic activity. *Sci. Reports.* **2018,** *8,* 1004.

Table 1. Amino acid sequences of Vc1.1 and analogues and inhibitory activity at α9α10 nAChR and $GABA_BR$-coupled $Ca_V2.2$ channels

		r = rat, h = human			
Vc1.1	GCCSDPRCNYDHPEIC*	28.3 (20.8~38.5) (r) 1000 (h)[24]	2.4 (0.8~7.0)	11.8 (r) 416.7 (h)	51.1±21.1
Vc1.1[N9R]	GCCSDPRC***R***YDHPEIC*	4901 (1729~13891) (r) 363 (306~427) (h)	4.9 (2.6~9.1)	1000 (r) 74.1 (h)	85.0±30.0
Vc1.1[N9R,D11N]	GCCSDPRC***R***Y***N***HPEIC*	13946 (8204~23707) (r)	>1000	<13.9 (r)	40.8±21.5
Vc1.1[N9R,D11S]	GCCSDPRC***R***Y***S***HPEIC*	ND	18.6 (6.3~55.1)		9.0±22.5
Vc1.1[N9R,D11R]	GCCSDPRC***R***Y***R***HPEIC*	ND	>1000		35.3±20.0
Benzoyl-Vc1.1[N9R]	***Benzoyl***-GCCSDPRC***R***YDHPEIC*	875 (511~1500) (r) 5929 (4519~8492) (h)	0.2 (0.1~0.3)	4375 (r) >25000 (h)	80.0±17.3
Ac-Vc1.1[N9R]	***Ac***-GCCSDPRC***R***YDHPEIC*	2416 (1462~3993) (r)	18.9 (7.9~45.5)	127.8 (r)	24.8±10.0
Δ-Gly-Vc1.1[N9R]	CCSDPRC***R***YDHPEIC*	ND	23.2 (11.1~48.6)		32.5±10.6
Benzoyl-Vc1.1	***Benzoyl***-GCCSDPRCNYDHPEIC*	12503 (8417~28510) (h)	1.2 (0.2~5.6)	>10000 (h)	

*C-terminus is amidated. The mutated residues are shown by bold and italic typeface. [#]Numbers in parentheses indicate 95% confidence intervals, n = 4-6. [##]Data are expressed as mean ± SD.

Figure Legends

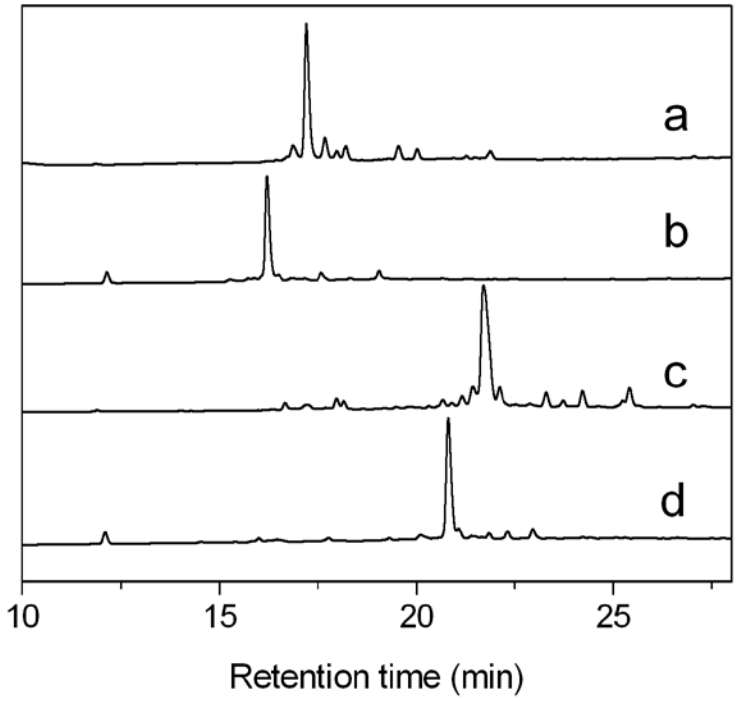

Figure 1. HPLC analysis of the folding of typical Vc1.1 variants. (a) Vc1.1[N9R] linear peptide and (b) Vc1.1[N9R] folded products, (c) Benzoyl-Vc1.1[N9R] linear peptide and (d) Benzoyl-Vc1.1[N9R] folded products. Samples were applied to a Calesil ODS-100 C_{18} column (4.6 × 250 mm) and eluted with a 25 min linear gradient of 5-60% acetonitrile (0.1% TFA) at flow rate of 1 mL/min.

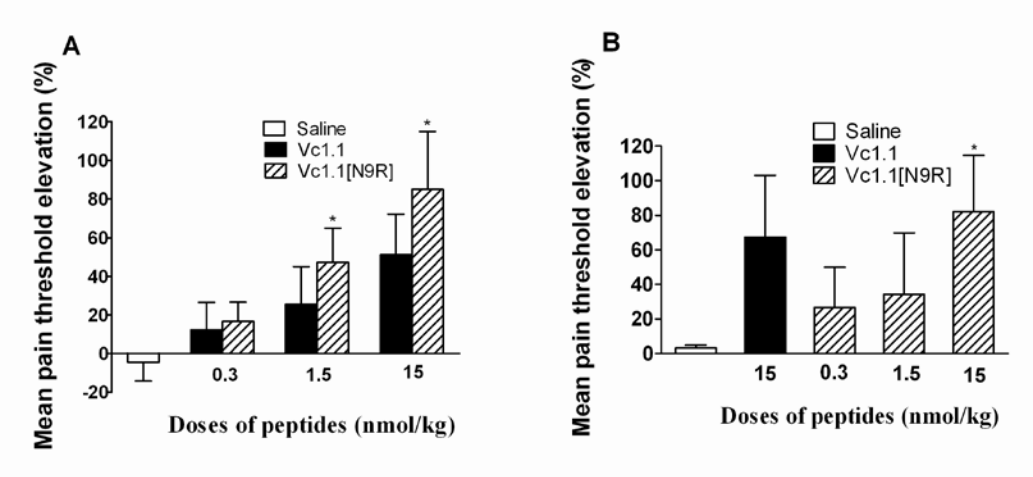

Figure 2. Analgesic activity of Vc1.1[N9R] in PNL and CCI rats. PNL rats (A) and CCI rats (B) (n = 8) were treated intramuscularly (i.m.) with saline, Vc1.1 (0.3, 1.5 and 15 nmol/kg) or Vc1.1[N9R] (0.3, 1.5 and 15 nmol/kg). The bar graph shows the mean pain threshold elevation percentage 2-2.5 h following i.m. injection. Data are expressed as mean ± SD.* $p <$ 0.05 compared with Vc1.1 group.

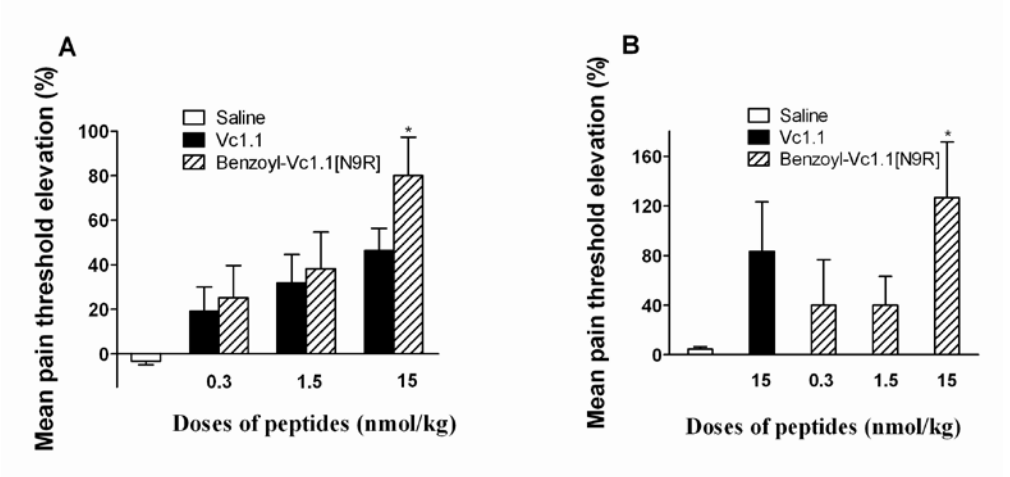

Figure 3. Analgesic activity of benzoyl-Vc1.1[N9R] in PNL and CCI rats. PNL rats (A) and CCI rats (B) (n=8) were treated intramuscularly with saline, Vc1.1 (0.3, 1.5 and 15

nmol/kg) or benzoyl-Vc1.1[N9R] (0.3, 1.5 and 15 nmol/kg). The bar graph shows the mean pain threshold elevation percentage 2-2.5 h following i.m. injection. Data are expressed as mean ± SD. * $p < 0.05$ compared with Vc1.1 group.

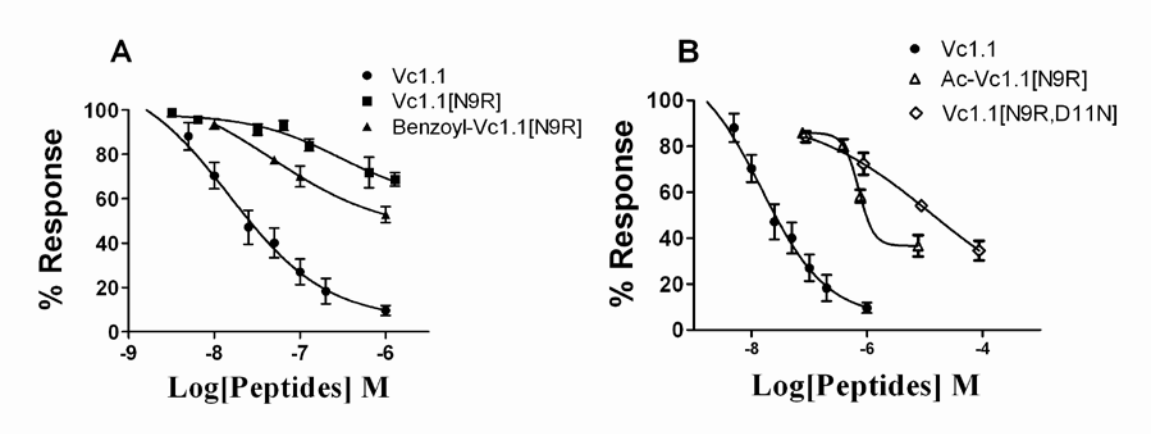

Figure 4. Effects of the key residues on the potency of Vc.1 at rat α9α10 nAChR. (A) The concentration-response relationship for inhibition of α9α10 nAChR by Vc1.1, Vc1.1[N9R] and benzoyl-Vc1.1[N9R] (n = 4-6); (B) The concentration-response relationship for inhibition of α9α10 by other Vc1.1 variants (n = 4-6). Peptides were applied by perfusion to oocytes expressing nAChRs as described in Materials and Methods. The error bars denote the SEM of the mean determined from four to six oocytes for each determination. The IC_{50} values obtained at the α3β2 nAChR subtype are summarized in Table 1.

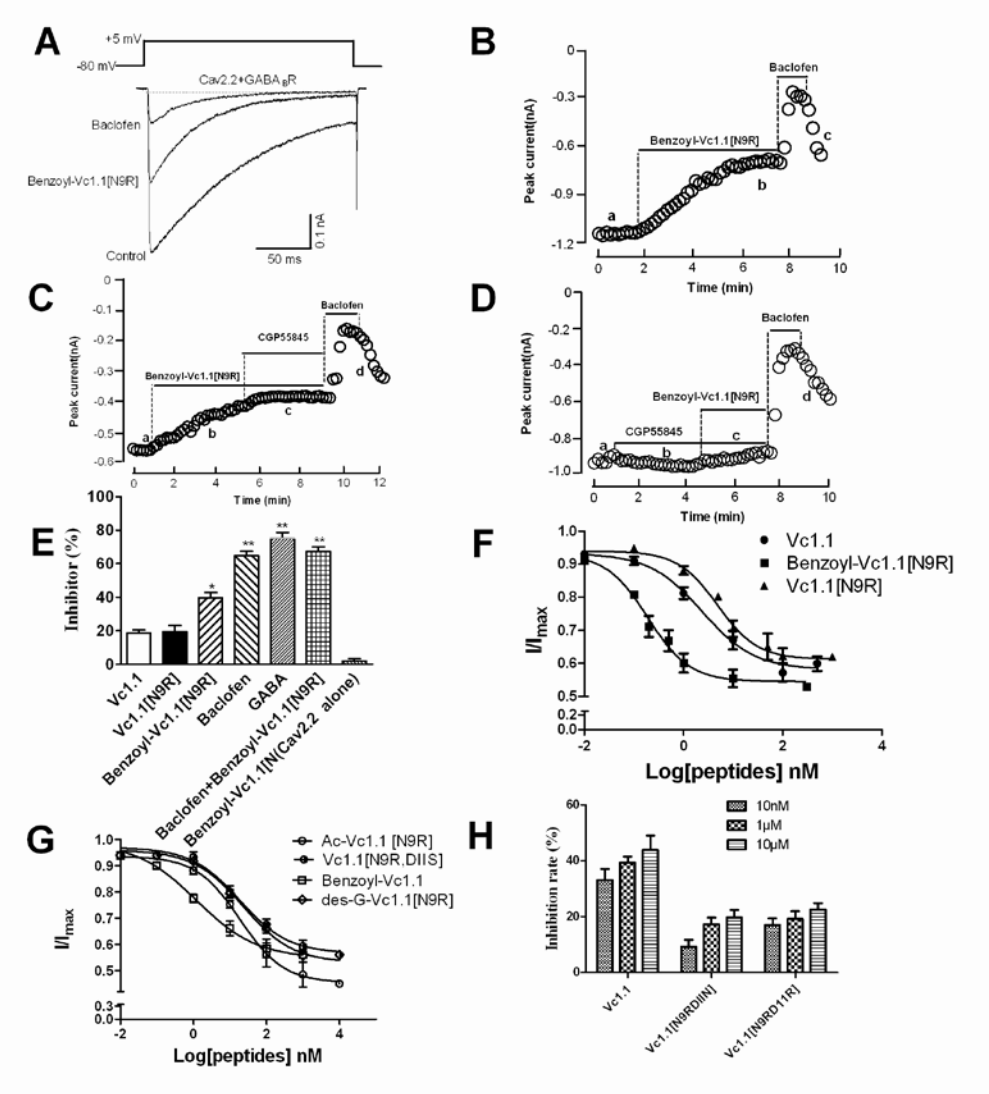

Figure 5. α-Conotoxin Vc1.1 variants, Vc1.1[N9R] and benzoyl-Vc1.1[N9R], inhibit $Ca_V2.2$ channels by activating $GABA_B$Rs in HEK293T cells. (A) Representative superimposed current traces from HEK293T cells co-expressing human $GABA_B$R and $Ca_V2.2$ channels in the absence and presence of benzoyl-Vc1.1[N9R] (1 nM) and baclofen (10 μM). (B) $GABA_B$Rs-coupled $Ca_V2.2$ inhibition of peak current amplitude by benzoyl-Vc1.1[N9R] (1 nM) and baclofen (10 μM) plotted as a function of time. (C) Representative time course of inhibition of peak current amplitude in the presence of benzoyl-Vc1.1[N9R] (1 nM), followed by application of the selective $GABA_B$ receptor antagonist, CGP55845 (1 μM). (D) Benzoyl-Vc1.1[N9R] exhibits no effect in the presence

of 1 μM CGP55845. (E) Bar graph of inhibition of peak Ba^{2+} current amplitude by 1 nM Vc1.1 (18.8 ± 4.1%), 1 nM Vc1.1[N9R] (19.6 ± 10.8%), 1 nM benzoyl-Vc1.1[N9R] (39.7 ± 9.4%), 10 μM baclofen (64.9 ± 5.1%), 10 μM GABA (75.3 ± 6.7%) in HEK203T cells co-expressing $GABA_BR$ and $Ca_V2.2$, 1 nM benzoyl-Vc1.1[N9R] plus 10 μM baclofen (67.4 ± 5.9%), and the effect of 10 μM benzoyl-Vc1.1[N9R] on $Ca_V2.2$ expressed alone (2.2 ± 2.1%). Data represent mean ± SEM (n = 4-6). *$p < 0.05$, **$p < 0.01$ versus Vc1.1, one-way analysis of variance. (F), (G) and (H) Concentration-response relationship for peptide inhibition of peak Ba^{2+} current in HEK293T cells co-expressing $GABA_BR$ and $Ca_V2.2$ channels. Data points represent averaged peak I_{Ba} amplitudes (I/Icontrol ± SEM); IC_{50} values obtained for Vc1.1 = 2.4 (0.8~7.0) nM, Vc1.1[N9R] = 4.9 (2.6~9.1) nM, and benzoyl-Vc1.1[N9R] = 0.2 (0.1~0.3) nM (n = 6–7 cells per data point). Numbers in parentheses indicate 95% confidence intervals, n = 4-6.

SUPPORTING INFORMATION

α-Conotoxin Vc1.1 variants target N-type Calcium channels via $GABA_B$ receptor activation and display improved analgesic activity

Fengtao Cai,[†,‡] Ning Xu,[†] Zhuguo Liu,[†] Rong Ding,[†] Shuo Yu,[†] Mingxin Dong,[†] Shuo Wang,[†] Jintao Shen,[†] Han-Shen Tae,[§] David J. Adams,[§,*] Xuerong Zhang[‡,*], Qiuyun Dai[*,†]

[†] Beijing Institute of Biotechnology; Beijing 100071, China

[‡] School of Preclinical Medicine, Guangxi Medical University, Nanning 530021, China

[§] Illawarra Health and Medical Research Institute (IHMRI), University of Wollongong, Wollongong, NSW 2522, Australia

Corresponding Author

*Phone: 86-10-66948897. Fax: 86-10-63833521. E-mail: qy_dai@yahoo.com; Xuerong Zhang, E-mail: zxrsv@126.com; David J. Adams, Email: djadams@uow.edu.au

Contents **Page**

Methods

Electrophysiological recording of TTX-S and TTX-R Na^+ currents in rat DRG neurons. Whole-cell voltage clamp recordings of voltage-gated sodium currents were made in rat DRG neurons which were acutely dissociated from 30-day old Sprague–Dawley rats and maintained in short-term primary culture according to the method described previously[1]. All methods and experimental protocols were approved and carried out in accordance with the guidelines and regulations of the Beijing Institutes for Biological Sciences Animal Research Advisory Committee. DRG neurons of large diameter (>35 μm) and those of relatively small diameter (<20 μm) were chosen for recording tetrodotoxin-sensitive (TTX-S) and tetrodotoxin-resistant (TTX-R) Na^+ currents, respectively. TTX (final concentration at 200 nM) was used to isolate TTX-R Na^+ currents from TTX-S Na^+ currents. Electrophysiological patch clamp recording was performed as described previously[2]. TTX-S and TTX-R Na^+ currents were evoked by a 50 ms depolarizing step to –10 mV and +10 mV, respectively, from a holding potential of –80 mV.

Oocyte two-electrode voltage clamp recording and data analysis of human α9α10 subtype. cRNA preparation, oocyte preparation and microinjection of human α9α10 nAChR were performed as described previously.[3] All procedures were approved by the University of Sydney Animal Ethics Committee.

Electrophysiological recordings were carried out 2–5 days post cRNA microinjection. Two-electrode voltage clamp recordings of *Xenopus. laevis* oocytes expressing human nAChRs were performed at room temperature (21−24 °C) using a GeneClamp 500B amplifier and pClamp9 software interface (Molecular Devices, Sunnyvale, CA, USA) at a holding potential −80 mV. Voltage-recording and current-injecting electrodes were pulled from GC150T-7.5 borosilicate glass (Harvard Apparatus, Holliston, MA) and filled with 3 M KCl, giving resistances of 0.3–1 MΩ.

Oocytes were incubated in 100 μM BAPTA-AM ~3 h before recording and perfused with ND115 solution containing (in mM): 115 NaCl, 2.5 KCl, 1.8 $CaCl_2$, and 10 HEPES at pH 7.4 using a continuous Legato 270 push/pull syringe pump perfusion system (KD Scientific, Holliston, MA, USA) at a rate of 2 mL/min in an OPC-1 perfusion chamber of < 20 μL volume (Automate Scientific, Berkeley, CA, USA). Due to the Ca^{2+} permeability of hα9α10 nAChRs, BAPTA-AM incubation was carried out to prevent the activation of *X. laevis* oocyte endogenous Ca^{2+}-activated chloride channels.

Initially, oocytes were briefly washed with ND115 solution followed by 3 applications of acetylcholine (ACh) at half-maximal effective concentration (EC_{50}) of ACh (6 μM) for human α9α10 nAChRs. Washout with bath solution was done for 3 min between ACh applications. Oocytes were incubated with peptides for 5 min with the perfusion system turned off, followed by co-application of ACh and peptide with flowing bath solution. All peptide solutions were prepared in ND115 + 0.1 % bovine serum albumin. Peak current amplitudes before (ACh alone) and after (ACh + peptide) peptide incubation were

measured using Clampfit version 10.7.0.3 software (Molecular Devices, Sunnyvale, CA, USA), where the ratio of ACh + peptide-evoked current amplitude to ACh alone-evoked current amplitude was used to assess the activity of the peptides at human α9α10 nAChRs. All electrophysiological data were pooled (n = 5-10) and represent means ± standard error of the mean (SEM). Data analysis was performed using GraphPad Prism 7 (GraphPad Software, La Jolla, CA, USA). The IC_{50} was determined from concentration-response relationships fitted to a non-linear regression function and reported with 95% confidence intervals.

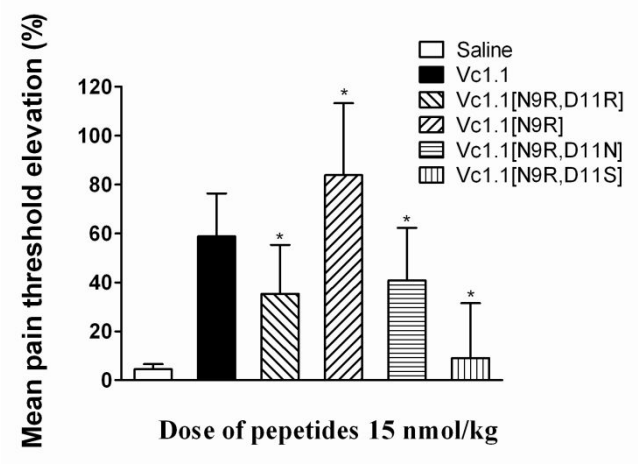

Figure S1. Analgesic activity of Vc1.1 variants at position 9 and 11 in PNL rats. PNL rats (n = 8/group) were treated intramuscularly (i.m.) with saline, Vc1.1, Vc1.1 [N9R,D11R], Vc1.1[N9R], Vc1.1[N9R,D11N] or Vc1.1[N9R,D11S]. The dose of peptide was 15 nmol/kg for all treatments. The bar graph shows the mean (SD) pain

threshold elevation percentage 2-2.5 h following i.m. injection. *p < 0.05 compared with Vc1.1 group.

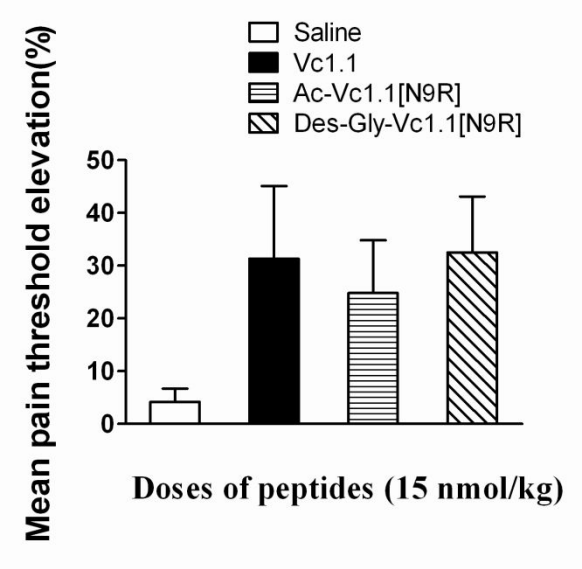

Figure S2. Analgesic activity of N-terminal modified Vc1.1[N9R] variants in PNL rats. PNL rats were treated intramuscularly with saline, Vc1.1, Ac-Vc1.1[N9R], or Des-Gly-Vc1.1[N9R] at 15 nmol/kg. The bar graph shows the mean ± SD pain threshold elevation percentage 2-2.5 h following i.m. injection of saline, Vc1.1, Ac-Vc1.1[N9R], and Des-Gly-Vc1.1[N9R]. p > 0.05 compared with Vc1.1 group.

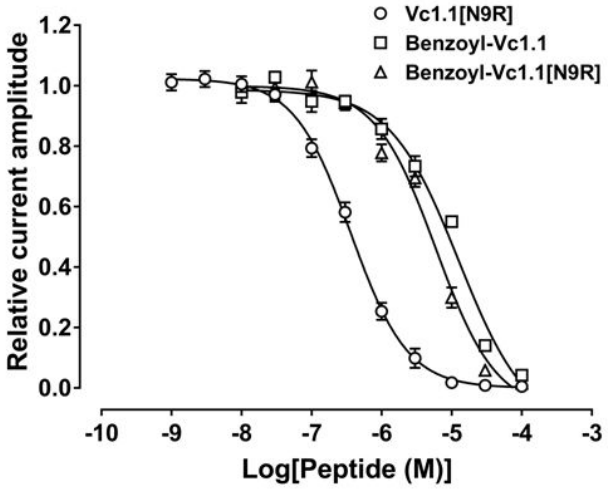

Figure S3. Concentration–response relationship for inhibition of human α9α10 nAChR by Vc1.1[N9R], benzoyl-Vc1.1 and benzoyl-Vc1.1[N9R]. The error bars denote the SEM of the mean determined from five to ten oocytes. The IC_{50} values obtained at the human α9α10 subtype are summarized in Table 1.

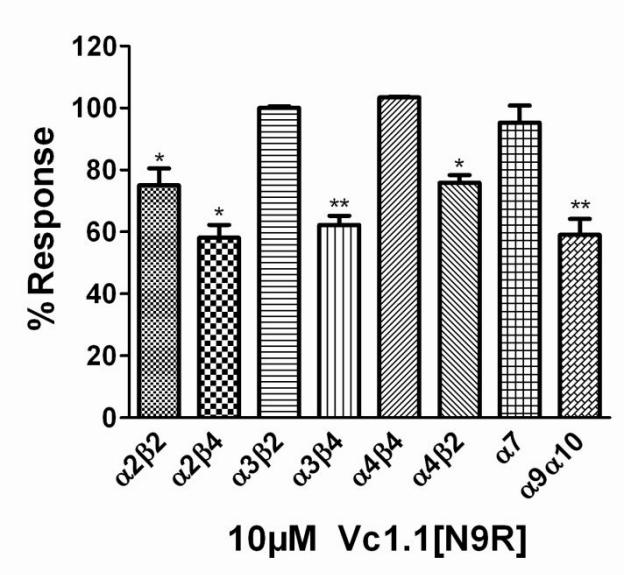

Figure S4. Vc1.1[N9R] inhibition of rat neuronal nAChR subtypes. Vc1.1[N9R] (10 μM) was applied by perfusion to oocytes expressing nAChRs as described in *Experimental section*. The error bars denote the SEM of the data from four to seven oocytes for each determination (n = 3-5).

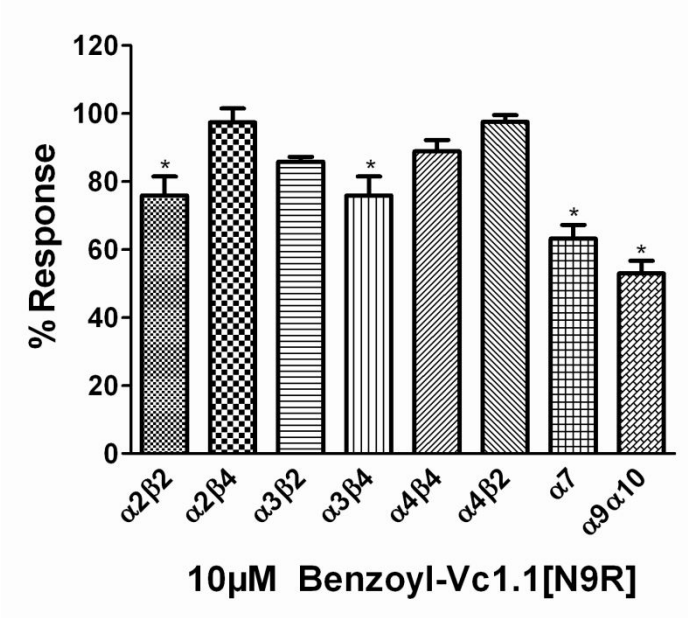

Figure S5. Benzoyl-Vc1.1[N9R] inhibition of rat nAChR subtypes. Benzoyl-Vc1.1[N9R] (10 μM) was applied by perfusion to oocytes expressing nAChRs as described in *Experimental section*. The error bars denote the SEM of the data from four to seven oocytes for each determination (n = 3-5).

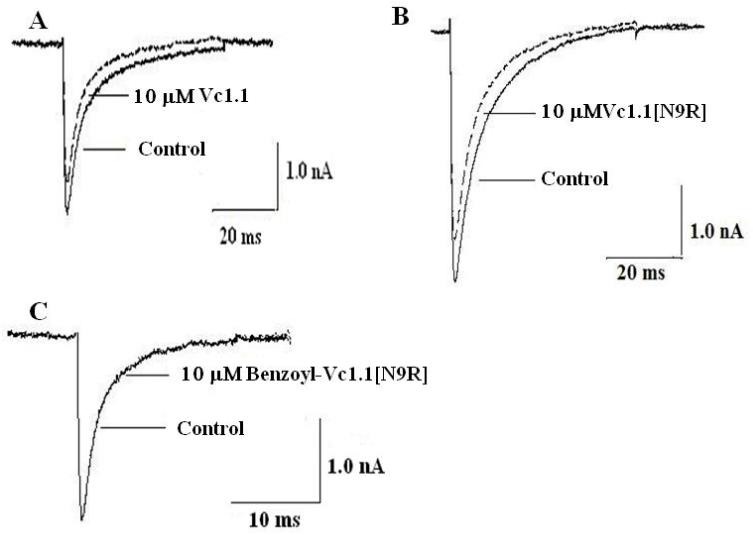

Figure S6. Effect of Vc1. 1, Vc1.1[N9R] and benzoyl-Vc1.1[N9R] (10 μM) on TTX-R Na^+ currents in rat DRG neurons (n = 4-6 for each). Superimposed TTX-R Na^+ currents were evoked by step depolarization (50 ms) to +10 mV from a holding potential of −80 mV in the absence (control) and presence of 10 μM Vc1.1 (A), 10 μM Vc1.1[N9R] (B), or 10 μM benzoyl-Vc1.1[N9R] (C).

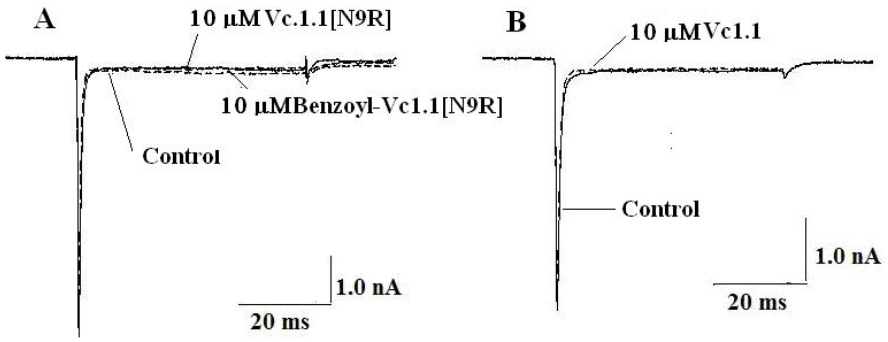

Figure S7. Effect of Vc1. 1, Vc1.1[N9R] and benzoyl-Vc1.1[N9R] (10 μM) on TTX-S Na^+ currents in rat DRG neurons (n = 4-6 for each). Superimposed TTX-S Na^+ currents

were evoked by step depolarization (50 ms) to −10 mV from a holding potential of −80 mV in the absence (control) and presence of 10 μM Vc1.1[N9R], 10 μM benzoyl-Vc1.1[N9R] (A) or 10 μM Vc1.1 (B).

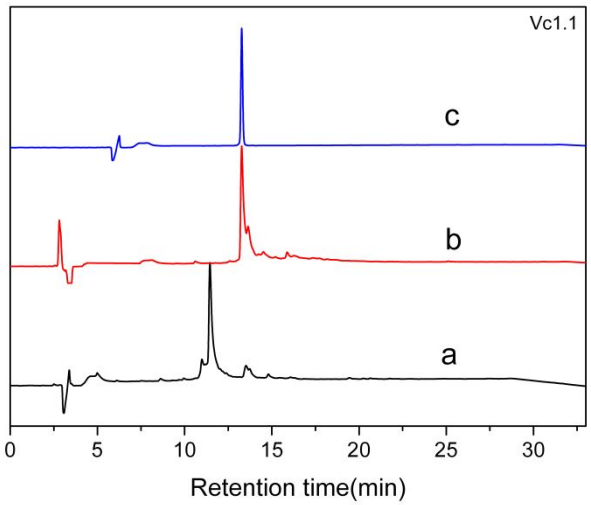

Figure S8. HPLC analysis of (a) linear, (b) folded, and (c) purified products of Vc1.1 (Purity: 99.8%)**.** Samples were applied to a Agilent Eclipse Plus C18 (5 μm, 4.6 mm×250 mm) and eluted with a linear gradient of 5-10% B for 0-1 min; 10~50% B (B is acetonitrile containing 0.1% TFA) for 1-25 min. Absorbance was monitored at 214 nm. Flow rate was 1.0 ml/min. a. linear Vc1.1; b. Vc1.1 folding products; c. Purified Vc1.1.

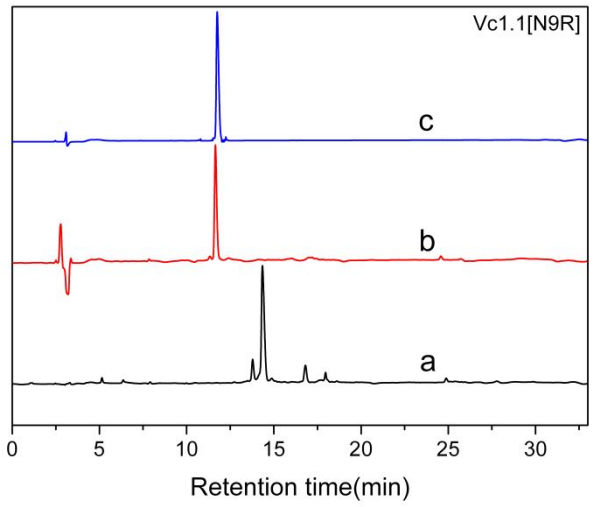

Figure S9. HPLC analysis of (a) linear, (b) folded, and (c) purified products of Vc1.1[N9R] (Purity: 98.0%)**.** Analytical conditions were the same as those described in Figure S8.

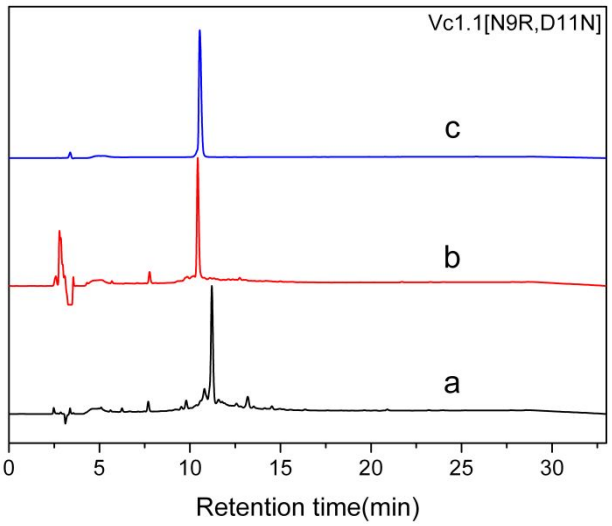

Figure S10. HPLC analysis of (a) linear, (b) folded, and (c) purified products of Vc1.1[N9R,D11N] (Purity: 96.9%). Analytical conditions were the same as those described in Figure S8.

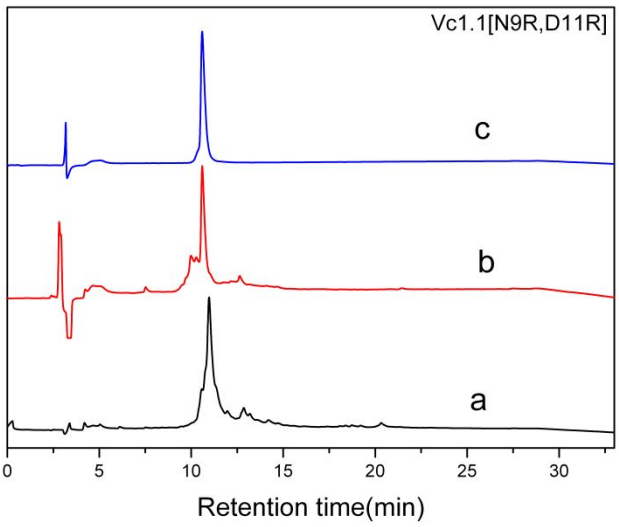

Figure S11. HPLC analysis of (a) linear, (b) folded, and (c) purified products of Vc1.1[N9R,D11R] (Purity: 95.0%)**.** Analytical conditions were the same as those described in Figure S8.

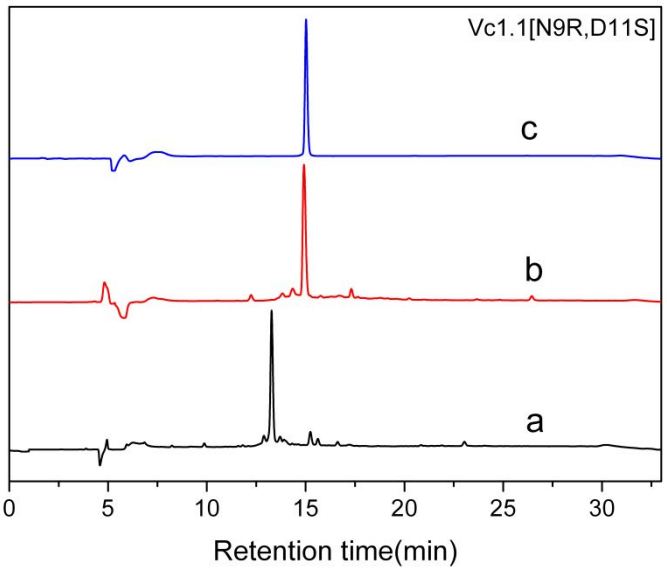

Figure S12. HPLC analysis of (a) linear, (b) folded, and (c) purified products of Vc1.1[N9R,D11S] (Purity: 97.8%). Analytical conditions were the same as those

described in Figure S8.

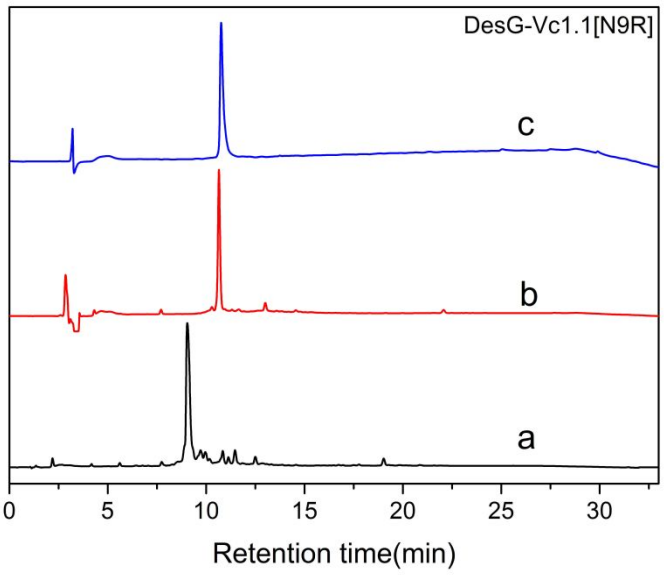

Figure S13. HPLC analysis of (a) linear, (b) folded, and (c) purified products of DesG-Vc1.1[N9R] (Purity: 100%). Analytical conditions were the same as those described in Figure S8.

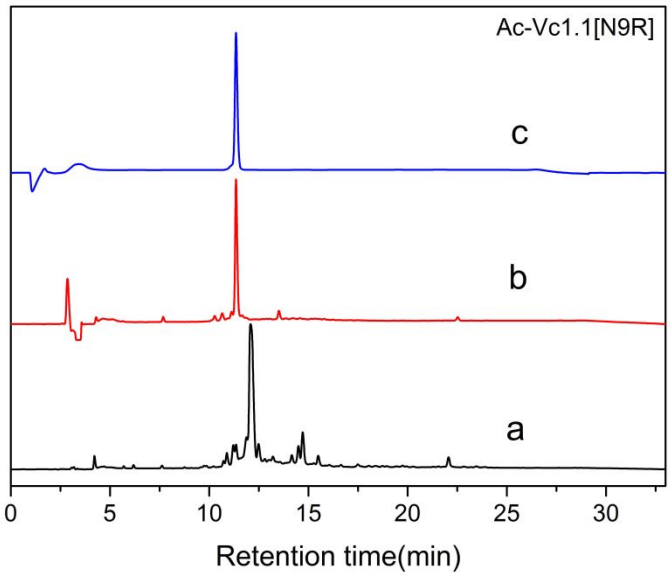

Figure S14. HPLC analysis of (a) linear, (b) folded, and (c) purified products of Ac-Vc1.1[N9R] (Purity: 96.5%)**.** Analytical conditions were the same as those described in Figure S8.

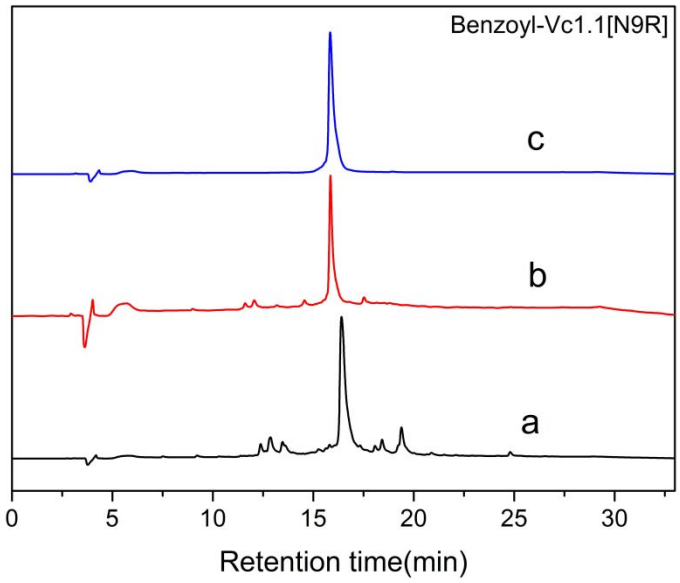

Figure S15. HPLC analysis of (a) linear, (b) folded, and (c) purified products of Benzoyl-Vc1.1[N9R] (Purity:97.6%). Analytical conditions were the same as those described in Figure S8.

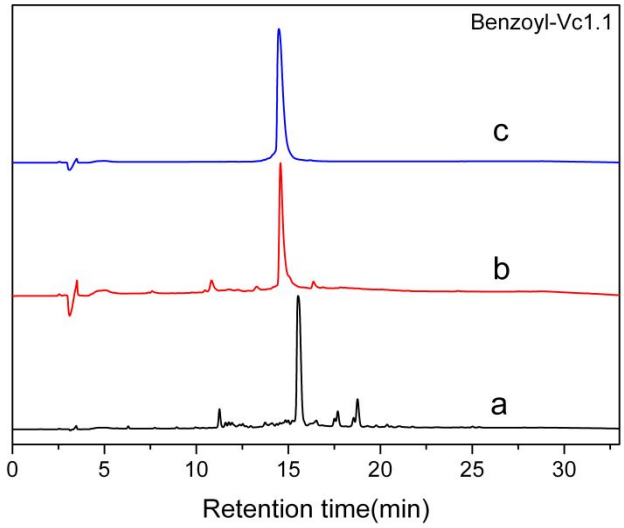

Figure S16. HPLC analysis of (a) linear, (b) folded, and (c) purified products of Benzoyl-Vc1.1(Purity: 95.2%). Analytical conditions were the same as those described in Figure S8.

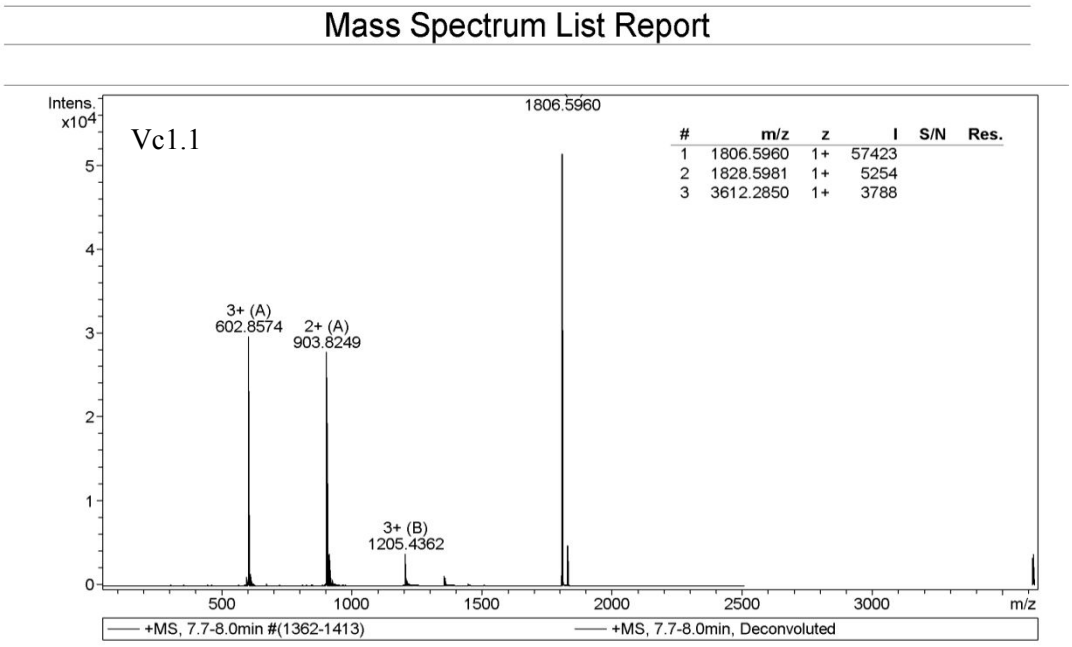

Figure S17. Mass spectrometry of Vc1.1

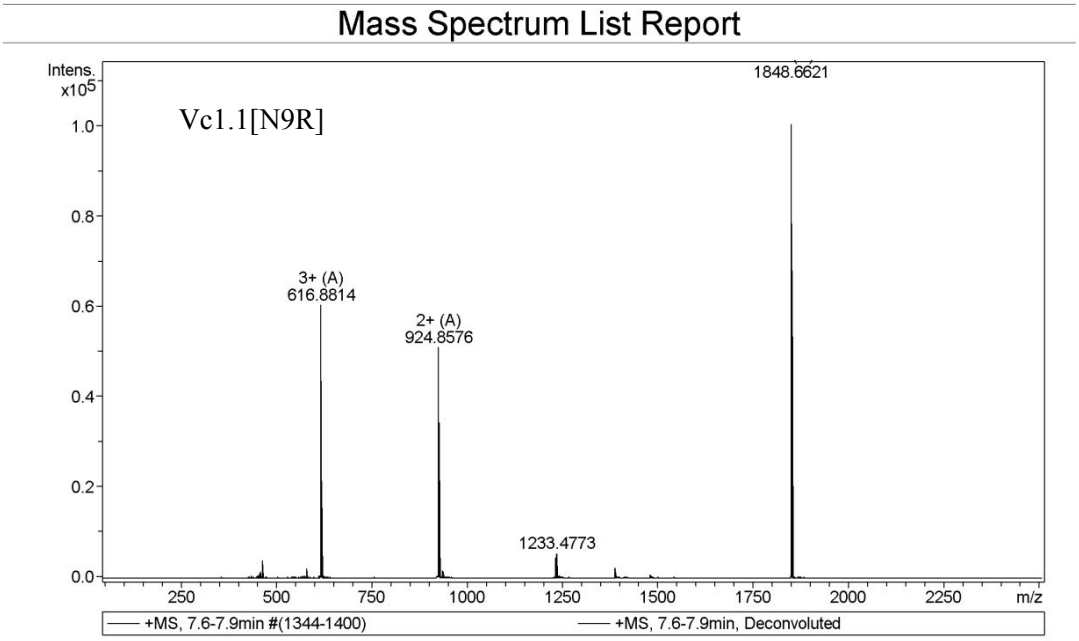

Figure S18. Mass spectrometry of Vc1.1[N9R]

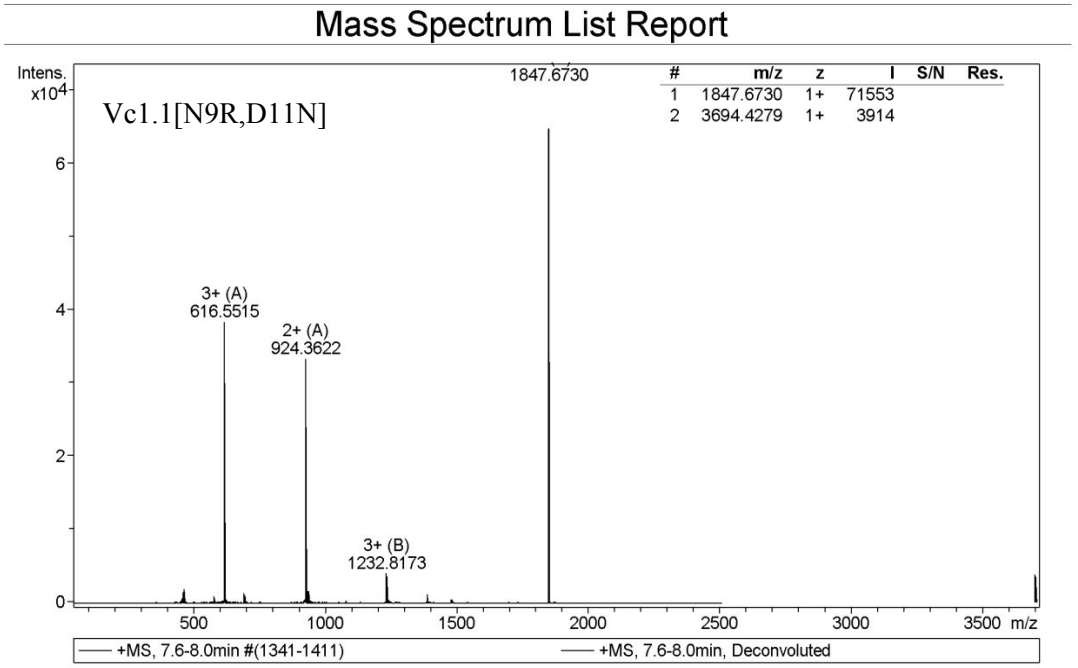

Figure S19. Mass spectrometry of Vc1.1[N9R,D11N]

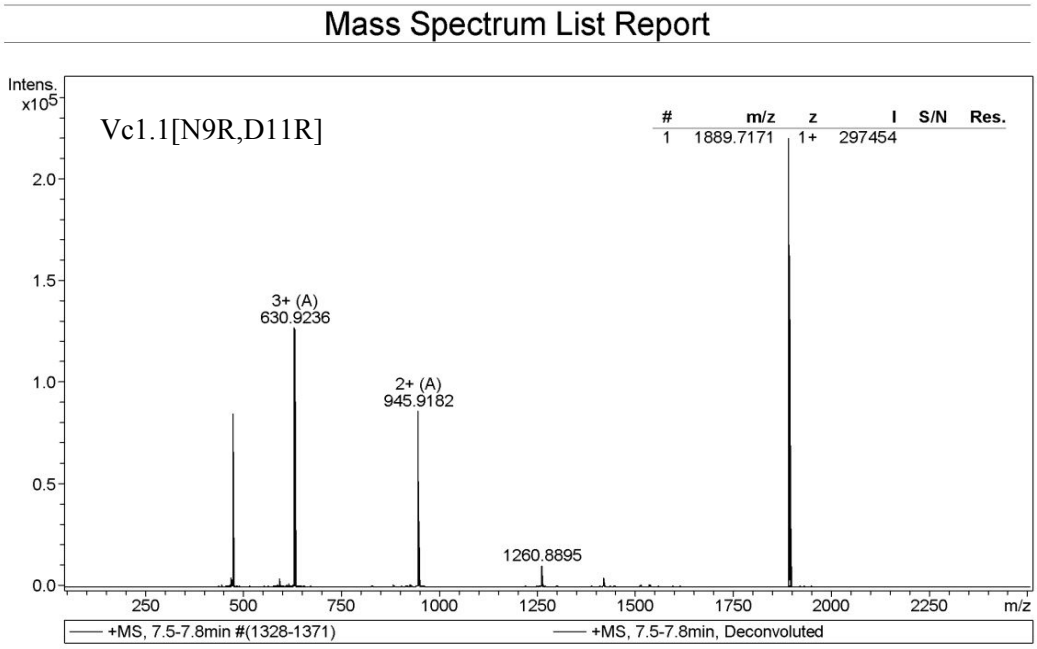

Figure S20. Mass spectrometry of Vc1.1[N9R,D11R]

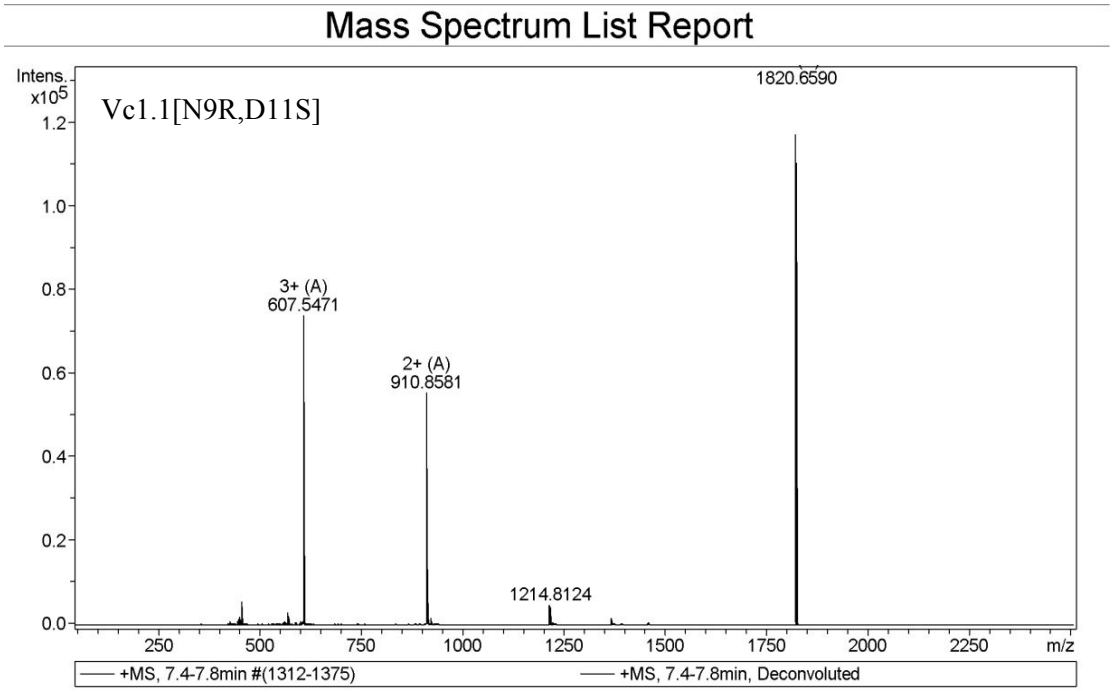

Figure S21. Mass spectrometry of Vc1.1[N9R,D11S]

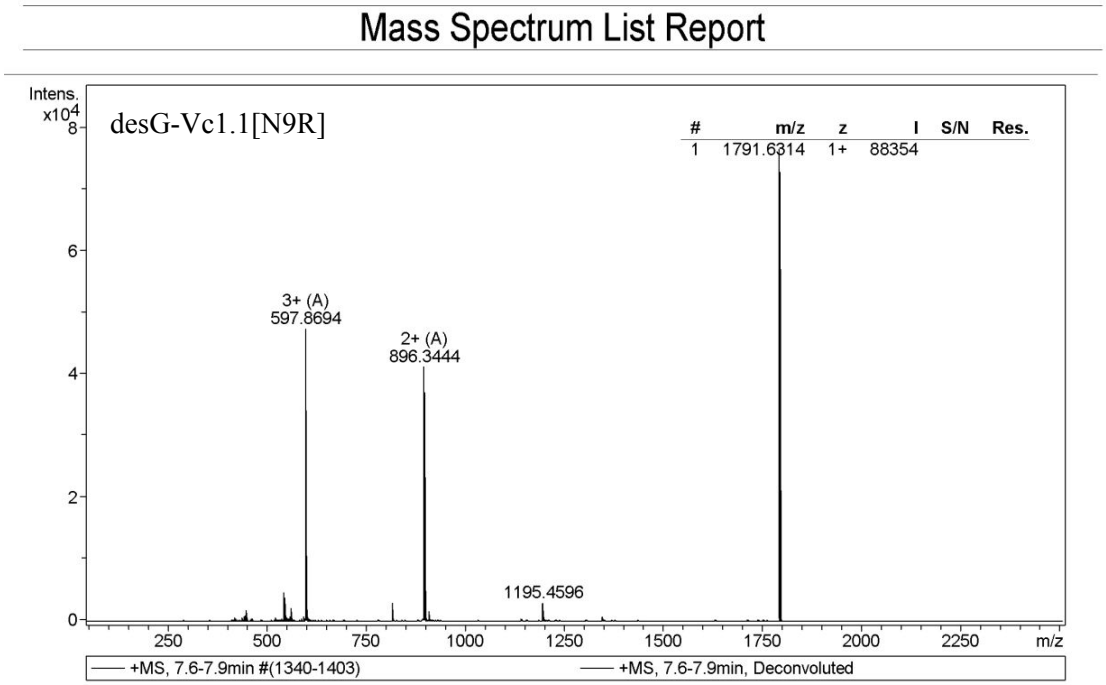

Figure S22. Mass spectrometry of DesG-Vc1.1[N9R]

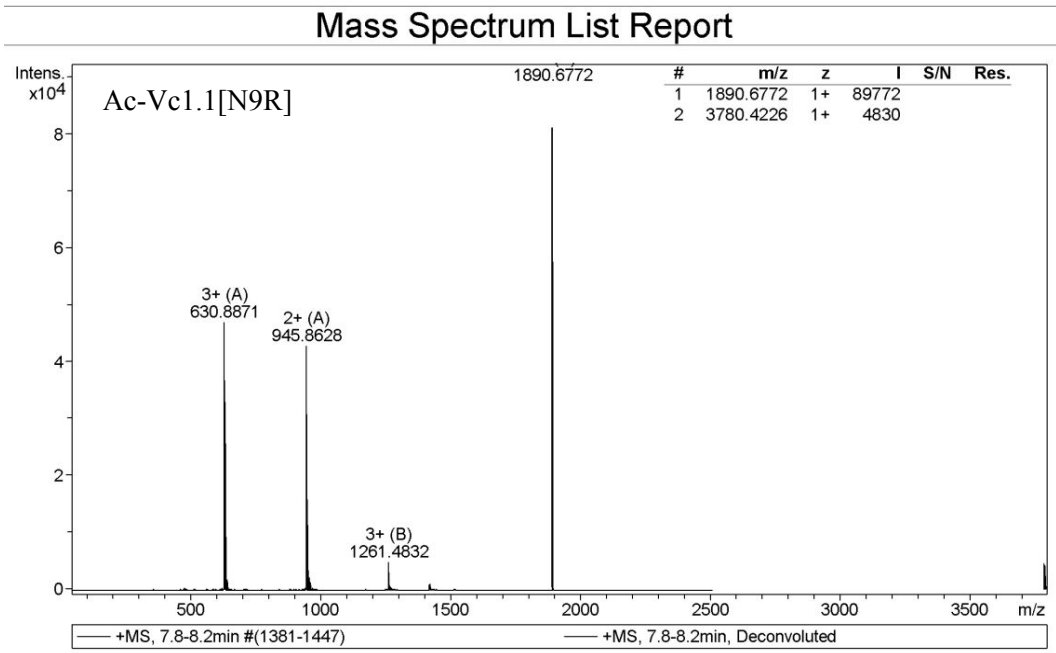

Figure S23. Mass spectrometry of Ac-Vc1.1[N9R]

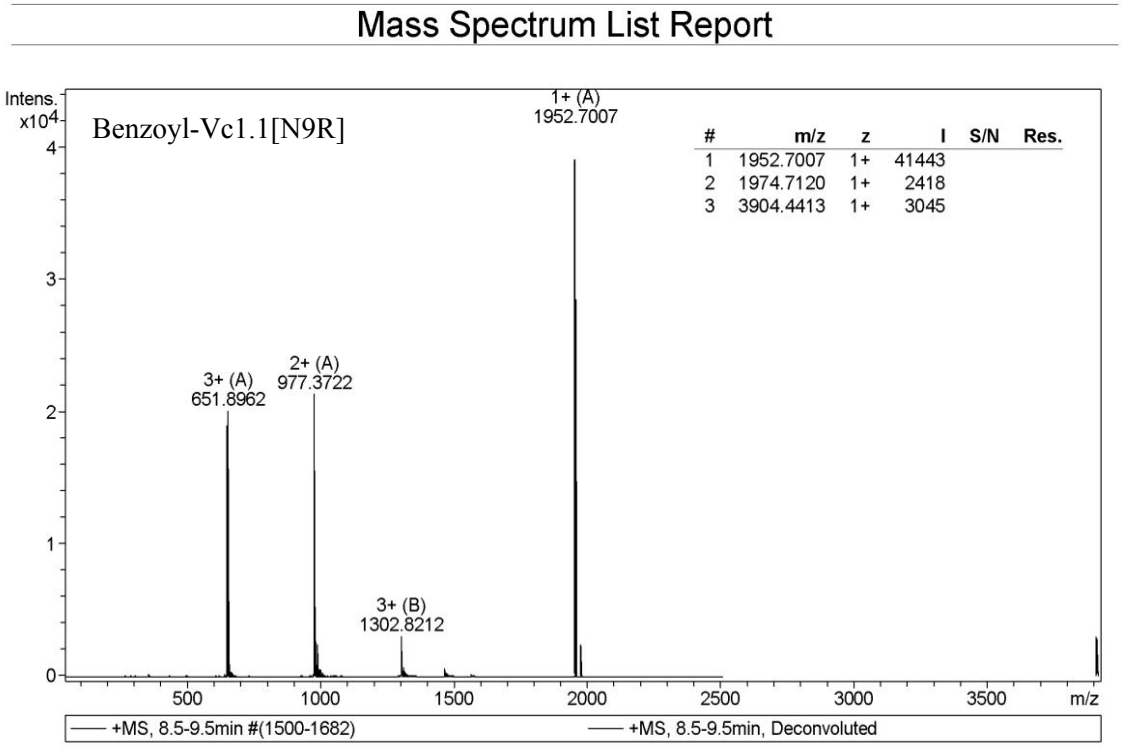

Figure S24. Mass spectrometry of benzoyl-Vc1.1[N9R]

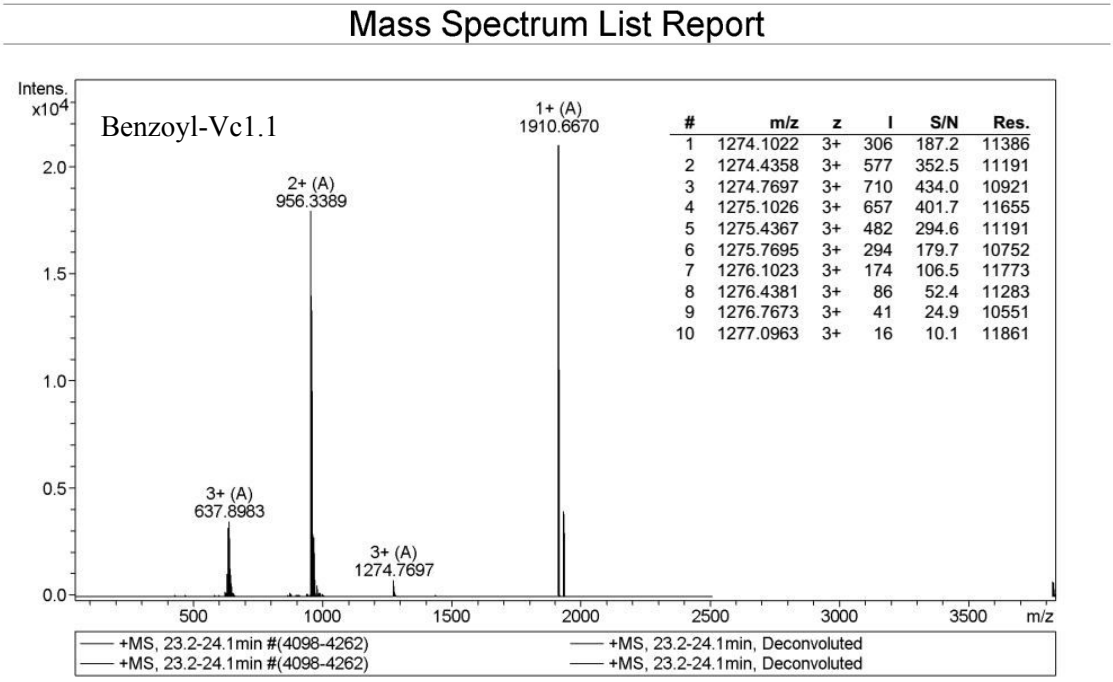

#	m/z	z	I	S/N	Res.
1	1274.1022	3+	306	187.2	11386
2	1274.4358	3+	577	352.5	11191
3	1274.7697	3+	710	434.0	10921
4	1275.1026	3+	657	401.7	11655
5	1275.4367	3+	482	294.6	11191
6	1275.7695	3+	294	179.7	10752
7	1276.1023	3+	174	106.5	11773
8	1276.4381	3+	86	52.4	11283
9	1276.7673	3+	41	24.9	10551
10	1277.0963	3+	16	10.1	11861

Figure S25. Mass spectrometry of benzoyl-Vc1.1

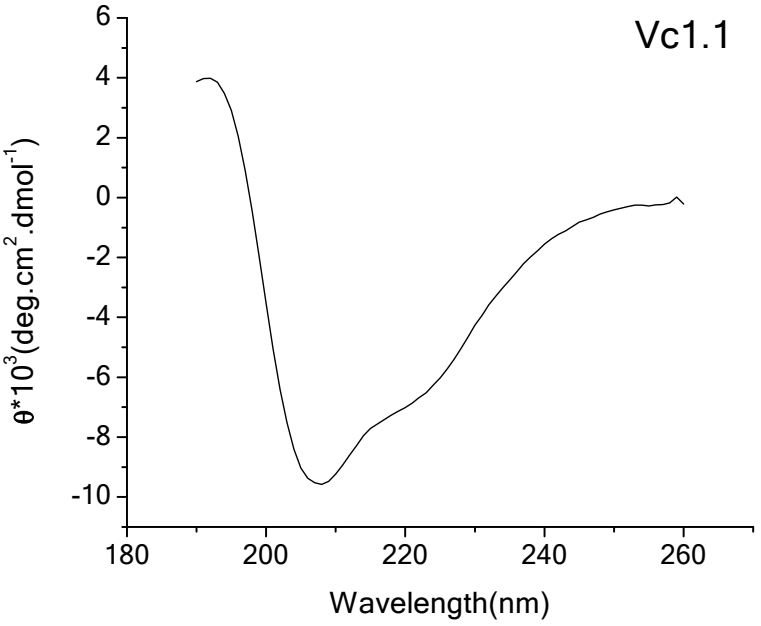

Figure S26. CD spectrum of Vc1.1

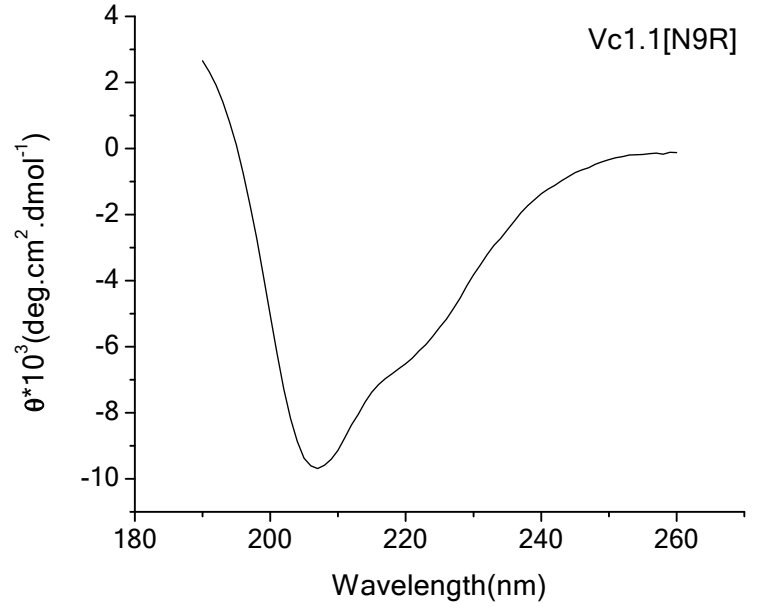

Figure S27. CD spectrum of Vc1.1[N9R]

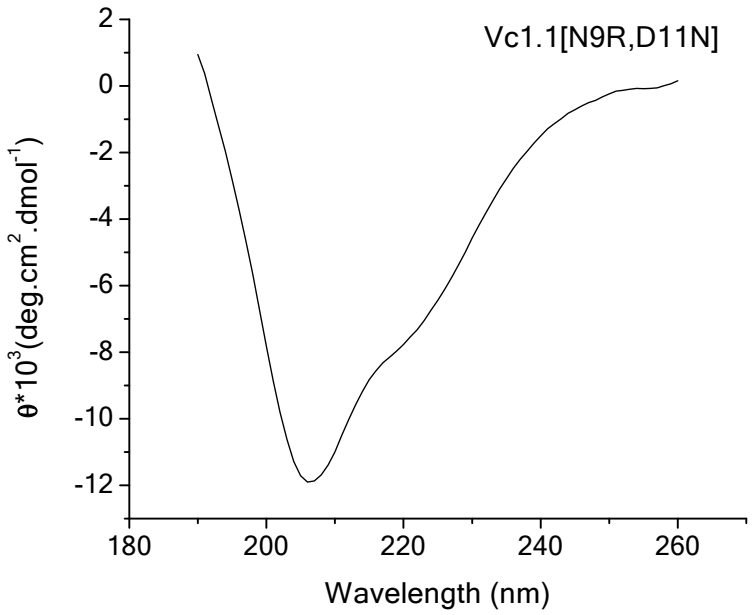

Figure S28. CD spectrum of Vc1.1[N9R,D11N]

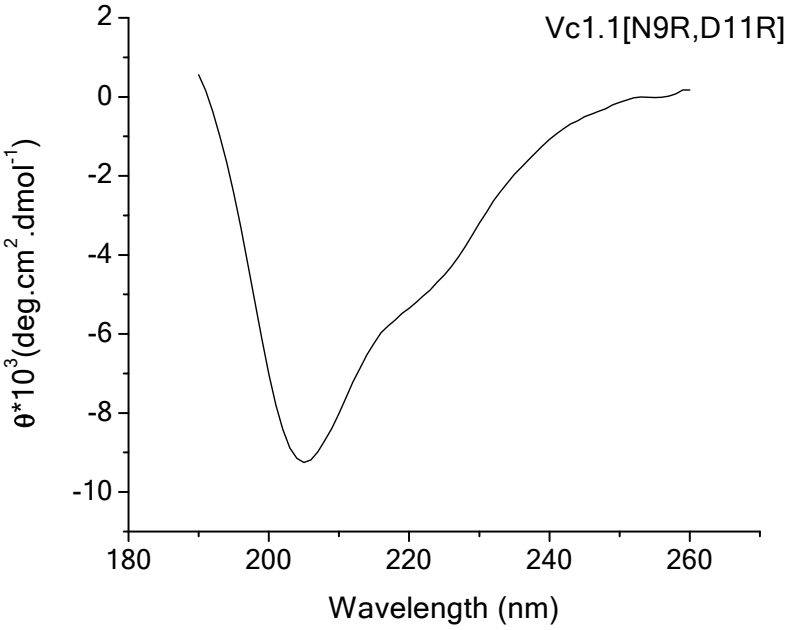

Figure S29. CD spectrum of Vc1.1[N9R,D11R]

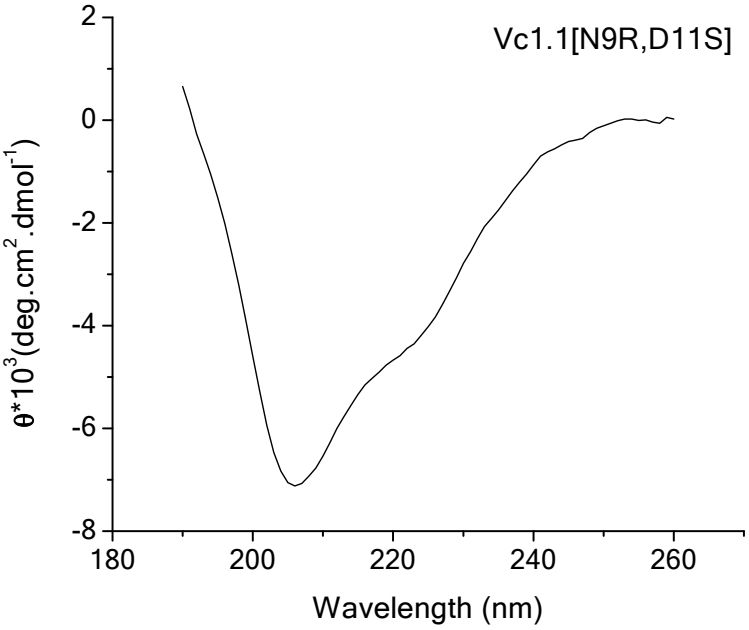

Figure S30. CD spectrum of Vc1.1[N9R,D11S]

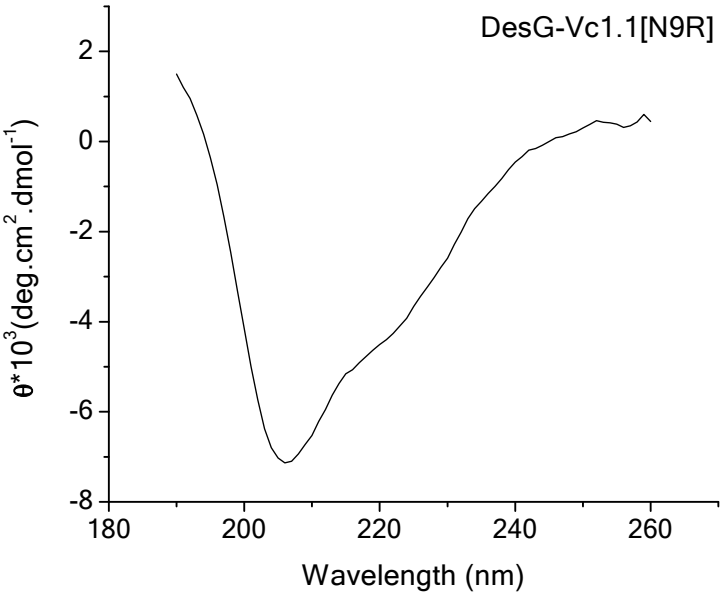

Figure S31. CD spectrum of DesG-Vc1.1[N9R]

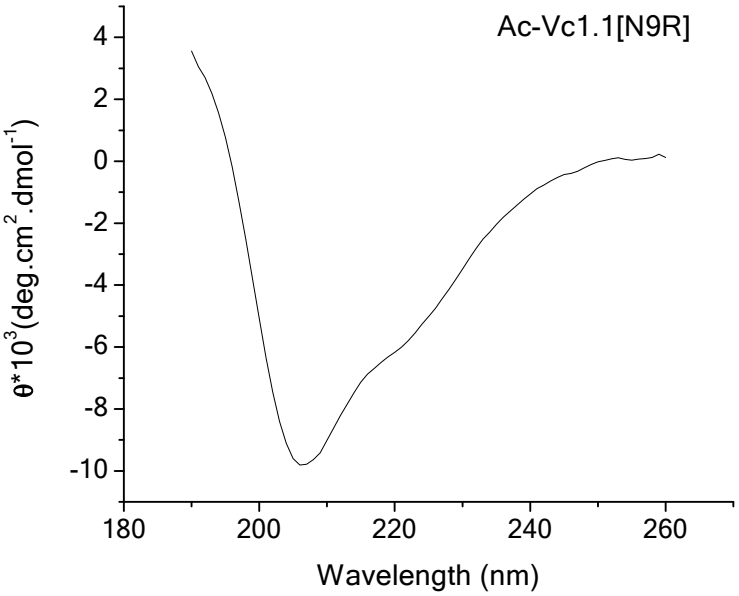

Figure S32. CD spectrum of Ac-Vc1.1[N9R]

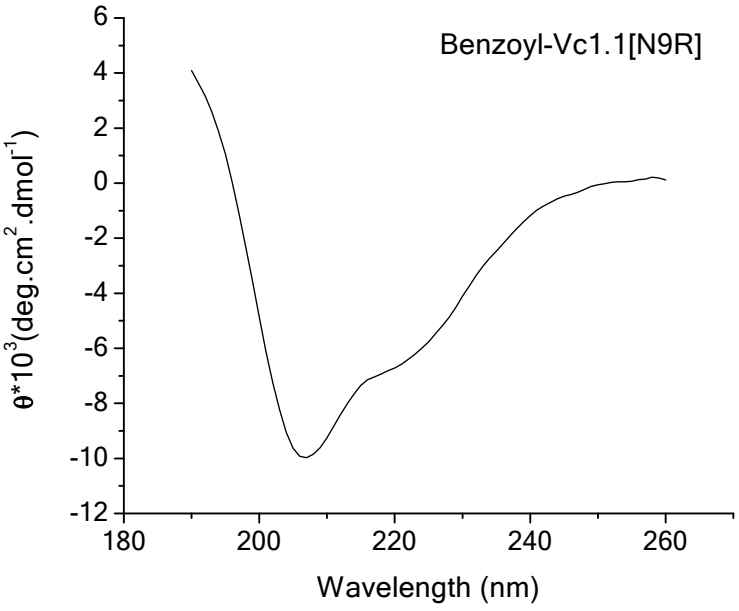

Figure S33. CD spectrum of benzoyl-Vc1.1[N9R]

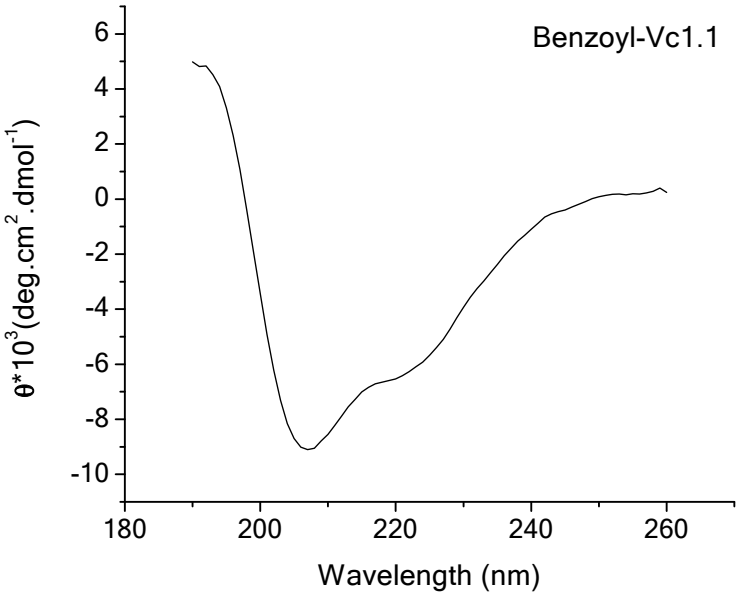

Figure S34. CD spectrum of benzoyl-Vc1.1

References

(1) Xiao, Y. C. & Liang, S. P. Inhibition of sodium channels in rat dorsal root ganglion neurons by Hainantoxin-IV, a novel spider toxin. *Sheng Wu Hua Xue Yu Sheng Wu Wu Li Xue Bao (Shanghai)* **2003**, *35***,** 82-85.

(2) Wang, H.; Zhang F.; Li, D.; Xu, S.; He, J.; Yu, H.; Li, J.; Liu, Z.; Liang, S. The venom of the fishing spider *Dolomedes sulfurous* contains various neurotoxins acting on voltage-activated ion channels in rat dorsal root ganglion neurons. *Toxicon* **2013**, *65***,** 68-75.

(3) Yu, R.; Tae, HS., Tabassum, N.; Shi, J.; Jiang, T.; Adams, D.J. Molecular determinants conferring the stoichiometric-dependent activity of α-conotoxins at the

human α9α10 nicotinic acetylcholine receptor subtype. *J. Med. Chem.* **2018**, 61, 4628-4634.